Journal of South American Earth Sciences 45 (2013) 293–315

Contents lists available at SciVerse ScienceDirect

Journal of South American Earth Sciences

journal homepage: www.elsevier.com/locate/jsames

Early Callovian ingression in southwestern Gondwana. Palaeoenvironmental evolution of the carbonate ramp (Calabozo Formation) in southwestern Mendoza, Neuquen basin, Argentina

Claudia Armella*, Nora G. Cabaleri, Mariana C. Cagnoni, Héctor O. Panarello

Instituto de Geocronología y Geología Isotópica, Consejo Nacional de Investigaciones, Científicas y Técnicas, Universidad de Buenos Aires, Pabellón INGEIS, Ciudad Universitaria, C1428EHA Buenos Aires, Argentina

ARTICLE INFO

Article history:
Received 15 November 2012
Accepted 21 March 2013

Keywords:
Carbonate ramp
Facies/microfacies analysis
Stable isotopes analysis
Callovian
Neuquén basin
Argentina

ABSTRACT

The carbonatic sequence of the Calabozo Formation (Lower Callovian) developed in southwestern Gondwana, within the northern area of the Neuquén basin, and is widespread in thin isolated outcrops in southwestern Mendoza province, Argentina. This paper describes the facies, microfacies and geochemical-isotopic analysis carried out in five studied localities, which allowed to define the paleoenvironmental conditions of a homoclinal shallow ramp model, highly influenced by sea level fluctuations, where outer, mid and inner ramp subenvironments were identified. The outer ramp subenvironment was only recognized in the south of the depocenter and is characterized by proximal outer ramp facies with shale levels and interbedded mudstone and packstone layers. The mid ramp subenvironment is formed by low energy facies (wackestone) affected by storms (packstones, grainstones and floatstones). The inner ramp subenvironment is the most predominant and is characterized by tidal flat facies (wackestones, packstones and grainstones) over which a complex of shoals (grainstones and packstones) dissected by tidal channels (packstone, grainstones and floatstones) developed. In the north area, protected environment facies were recorded (bioturbated wackestones and packstones). The vertical distribution of facies indicates that the paleoenvironmental evolution of the Calabozo Formation results from a highstand stage in the depocenter, culminating in a supratidal environment, with stromatolitic levels interbedded with anhydrite originated under restricted water circulation conditions due to a progressive isolation of the basin. $\delta^{13}C$ and $\delta^{18}O$ values of the carbonates of the Calabozo Formation suggest an isotopic signature influenced by local palaeoenvironmental parameters and diagenetic overprints. The $\delta^{13}C$ and $\delta^{18}O$ oscillations between the carbonates of the different studied sections are related with lateral facies variations within the carbonate ramp accompanied with dissimilar reactivities in relation to diagenetic fluids. The $\delta^{18}O$ values of all sections exhibit a rather broad scatter which may be attributed to diagenesis and recrystallisation while the carbon isotopic composition has been less affected by those processes. Carbon isotope system has best retained the primary isotopic signal and $\delta^{13}C$ values (0–3.9‰) are within the Callovian isotope range. The $^{87}Sr/^{86}Sr$ ratios of the bulk carbonates of El Plomo creek, La Vaina creek and Potimalal River sections are in agreement with the Callovian seawater Sr-isotope curve.

1. Introduction

The Calabozo Formation (Dessanti, 1973) represents the carbonate ramp developed on the southwestern margin of Gondwana which records the eocallovian ingression in the northern area of the Neuquén basin, Argentina.

During the Early Callovian the basin recorded a clear reduction of the depocenter and the progradation of marginal marine facies (Legarreta and Uliana, 1996, 1999). After the eocallovian ingression, the marine conditions settled in the southwestern Mendoza favoured carbonate deposition in areas with scarce detrital input. Therefore, Calabozo Formation characterizes the change from detrital to carbonate sedimentation and the study of its paleoenvironmental evolution reveals the progressive restriction of the depocenter. Furthermore, this sequence records the last marine ingression of the first transgressive-regressive cycle developed in the Neuquén basin.

* Corresponding author. Tel./fax: +54 11 4783 3024.
E-mail addresses: armella@ingeis.uba.ar, claudia.armella@gmail.com (C. Armella), cabaleri@ingeis.uba.ar (N.G. Cabaleri), mariana@ingeis.uba.ar (M.C. Cagnoni), hector@ingeis.uba.ar (H.O. Panarello).

0895-9811/$ – see front matter © 2013 Elsevier Ltd. All rights reserved.
http://dx.doi.org/10.1016/j.jsames.2013.03.013

The Calabozo Formation is characterized by isolated outcrops less than 20 m thick exposed in southwestern Mendoza, from the Salado river to the south of Bardas Blancas (Fig. 1).

While bibliography on the analysis of Jurassic-Cretaceous sequences in the region is vast, background data regarding the Calabozo Formation is scarce, since Bathonian-Eocallovian deposits have been seldom described throughout literature due to their restricted areal distribution. First to mention these sequences was Dessanti (1973, 1978), who described the carbonatic beds in Calabozo creek and near Puchenque hill, with the name of Calizas del Calabozo Formation. According to him the unit was Oxfordian in age probably because he included beds of La Manga Formation within the sequence (Legarreta and Gulisano, 1989; Legarreta et al., 1993). Afterwards, on the basis of the ammonite fauna from the type section Riccardi (1984), Riccardi and Westermann (1991) and Legarreta et al. (1993), assigned to the Calabozo Formation an Early Callovian age. This age was confirmed in later works by Legarreta et al. (1999), Leanza et al. (2000) and Riccardi et al. (1999, 2000), based on new stratigraphic and palaeontologic information.

This paper focuses on facies/microfacies analysis and geochemical–isotopic data from detailed stratigraphic sections located in the Serrucho creek, Calabozo creek, El Plomo creek, La Vaina creek and Potimalal river areas (Fig. 1). Some preliminary studies have been published by Cabaleri et al. (2001, 2003), Valencio et al. (2003), Armella et al. (2005a) and Cagnoni et al. (2006). The aims of this paper are the palaeoenvironmental and palaeogeographic reconstructions of the southwestern margin of Gondwana during the Early Callovian in a previously poorly documented carbonate ramp context.

2. Geological setting

The Neuquén basin is a Mesozoic back-arc rift basin developed on the southwestern convergent margin of the South American plate, in west central Argentina and eastern Chile between 34°–41° S and 66°–71° W. It lies within four Argentine provinces: Mendoza, Rio Negro, Neuquén and La Pampa. The Neuquén basin has a broadly triangular shape with a narrow N–S elongated strip, restricted to the Andean belt, between 34° and 37° S.

The geologic evolution of the basin was controlled by the active subduction and development of the magmatic arc along the western margin of Gondwana. The highly complex history of the basin is characterized by the development of syn-rift (Late Triassic–Pliensbachian), post-rift (Pliensbachian-Barremian) and foreland stages (Legarreta and Gulisano, 1989; Howell et al., 2005). During the syn-rift phase in the northern area of the Neuquén basin, a series of half grabens trending NNW–ESE were developed and filled by volcanic and sedimentary sequences (Precuyano Cycle; Gulisano, 1981) in isolated depocenters (Uliana and Biddle, 1988; Uliana et al., 1989, 1995). During the Pliensbachian, the subsidence of the back-arc allowed marine expansion, flooding the basin through gaps in the magmatic arc (Spalletti et al., 2000) and connecting the depocenters (Giambiagi et al., 2009). At first, sedimentation was strongly influenced by the topography inherited from the syn-rift stage (Burguess et al., 2000; Mc ILroy et al., 2005; Cristallini et al., 2009). The basin stratigraphy is characterized by a thick sedimentary sequence (more than 7000 m) accumulated from the Late Triassic to the Paleocene age but most of the sediments were deposited during the post-rift phase; which comprises the Cuyo, Lotena and Mendoza groups (Legarreta and Gulisano, 1989) (Fig. 2). The palaeogeographic reconstruction of the basin during Jurassic and Cretaceous combining surface, subsurface and seismic data, indicates a connection with the Proto-Pacific Ocean during these periods (Legarreta et al., 1993; Legarreta and Uliana, 1999). Regional geological background can be found in papers by Gulisano and Gutiérrez Pleimling (1995), Legarreta and Uliana (1999), Riccardi et al. (2000) and Franzese and Spalletti (2001) among others.

In southwestern Mendoza, palaeogeography and sedimentation were controlled by tectonic processes and sea level variations. Consequently, a complex depositional pattern developed, where repeated interbeddings of detrital, carbonatic and evaporitic sedimentation conditions can be observed (Legarreta and Uliana, 1996, 1999). The expansion of the basin coincided with the beginning of a long-term stage of subsidence, during which marginal and marine sediments of the Cuyo Group were deposited (Groeber, 1946; Gulisano et al., 1984; Leanza, 2009; Arregui et al., 2011).

The Cuyo Group (Groeber, 1946; Groeber et al., 1953; Digregorio and Uliana, 1980) or Cuyo Mesosequence (Legarreta and Gulisano, 1989) from Late Hettangian – Callovian age, represents the first

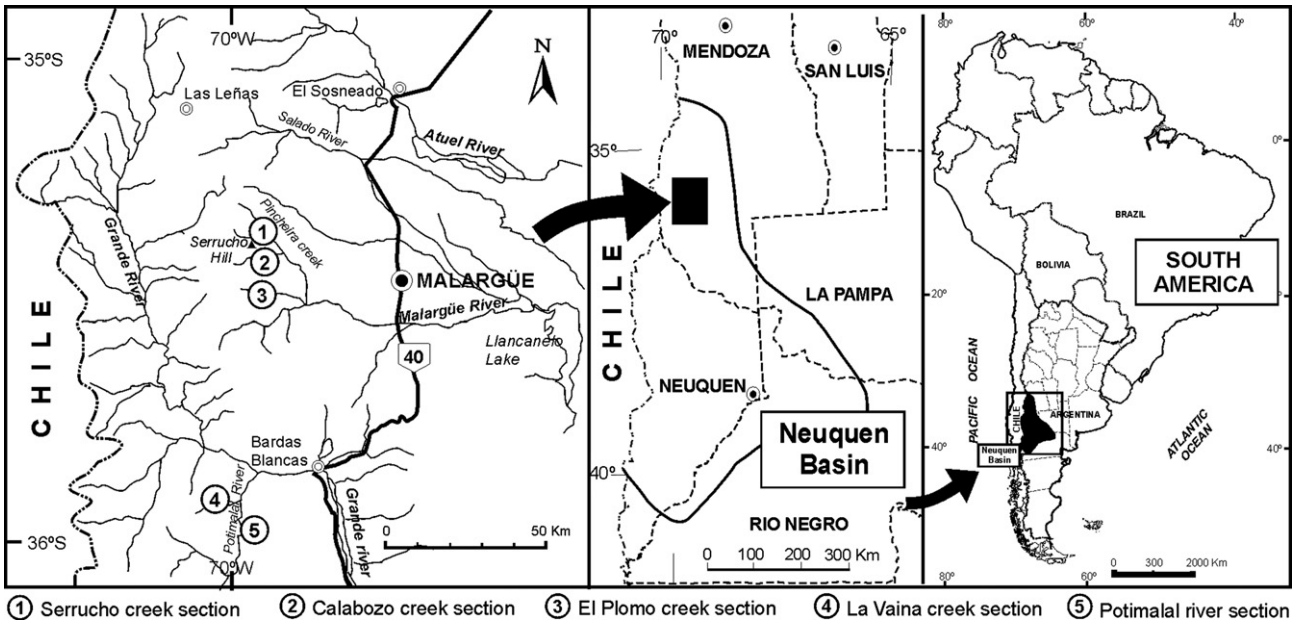

Fig. 1. Studied area at the northwestern Neuquén basin showing the localities where sampling was carried out.

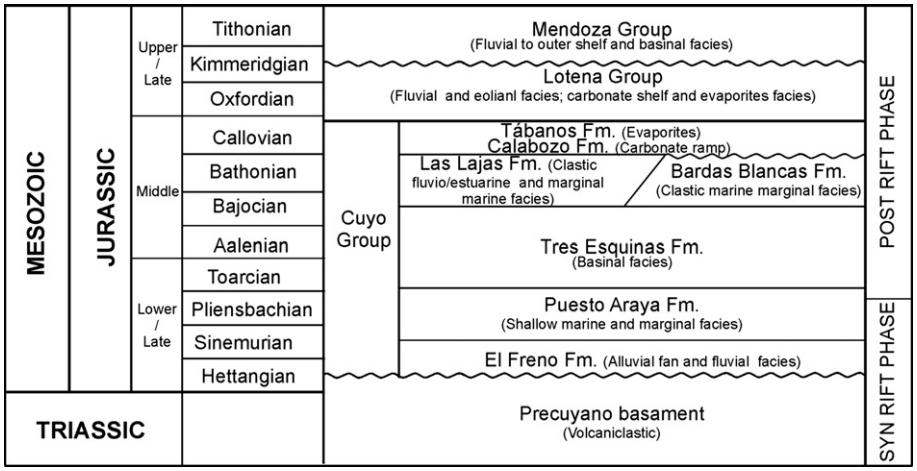

Fig. 2. Stratigraphic chart of the Jurassic succession of the northwestern Neuquén basin (southwestern Mendoza). Adapted from Gulisano and Gutiérrez Pleimling (1995); Legarreta and Gulisano (1989); Legarreta and Uliana (1999); Mazzini et al. (2010) and Leanza et al. (2012).

transgressive-regressive cycle of the basin, revealing a clear influence of the eustatic sea level changes (Leanza et al., 2000). In southwestern Mendoza, sedimentation began with continental deposits of alluvial fan and fluvial facies of El Freno Formation (Yrigoyen, 1979; Gulisano, 1981) which pass to fan-deltaic sediments and shallow marine facies of Puesto Araya Formation (Volkheimer, 1970). The deeper marine and euxinic sea bottom facies are represented by the Tres Esquinas Formation (Stipanicic, 1969). Later studies of Mazzini et al. (2010) and Leanza et al. (2012) identified evidences of the Toarcian Oceanic Anoxic Event in basal levels of Tres Esquinas Formation in Serrucho creek outcrops (La Valenciana depocenter) and they also brought new radiometric U–Pb ages from Early Jurassic ash layers. The Tres Esquinas Formation is capped by sandy fluvio-estuarine facies of the prograding Lajas Formation (Weaver, 1931; Gulisano and Hinterwimmer, 1986) which was the result of a sudden sea level fall in the Late Bajocian (Gulisano and Gutiérrez Pleimling, 1995).

During Early Callovian, shallow marine facies in the west of Malargüe prograded into the basin providing a suitable setting for the distinctive carbonatic sedimentary regime of the Calabozo Formation. The carbonate facies association of this unit indicates that the depocenter was far away from the areas of detrital input and was controlled by the topography inherited from the former depositional system (Legarreta and Uliana, 1996). Calabozo Formation conformably overlies the siliciclastic succession of the Lajas Formation, while in the south of Bardas Blancas; it is in erosive contact with the on-shore sandy facies of Bardas Blancas Formation (Gulisano, 1981; Legarreta et al., 1993).

Calabozo Formation limestones change gradually to the evaporitic sequence of Tábanos Formation (Lower Callovian) (Stipanicic, 1966; Dellape et al., 1979). These anhidrite deposits reveal the dessication of the basin (Legarreta and Uliana, 1996, 1999; Legarreta, 2002), and reflect isolated conditions from the Pacific Ocean, and a depocenter reduction, probably due to the effect of the magmatic arc activity on the western margin of Gondwana.

3. Methodology

This study deals with a sedimentological analysis based on detailed field observations and sampling made along five profiles in the Calabozo Formation, from north to south to the eocallovian depocenter: Serrucho creek, Calabozo creek, El Plomo creek, La Vaina creek and Potimalal river (Fig. 1). We also identified facies associations and stratigraphic architecture of the deposits. Sedimentary structures were examined on a cm/dm scale. An orientated sample collection (14 samples from Serrucho creek, 11 from Calabozo creek, 26 from El Plomo creek, 30 from La Vaina creek and 27 from Potimalal river) was made in order to perform thin sections and polished surfaces for the study of facies/microfacies and post-depositional features, followed by semi-quantitative components analysis. Samples and thin sections were stained with calcium ferricyanide and alizarin red-s to distinguish carbonate minerals (Flügel, 2004; Adams et al., 1995). Microfacial data were obtained in thin sections of 7.5 cm^2 by quantitative analyses. Facies and microfacies classification and their environmental interpretation were based on texture, fabric, bioclasts, intrabasinal and extrabasinal grains amounts, sedimentary structures, bioturbations and hydrodynamism (Wilson, 1975; Read, 1985; Tucker and Wright, 1990; Wright and Burchette, 1996; Flügel, 2004). Correlation between outcrop areas was based on facies analysis and their environmental implications.

To carry out isotopic analyses we selected the better preserved carbonates on the basis of petrographic and geochemical studies. Carbon and oxygen isotope and trace elements analyses presented in this paper were performed at INGEIS on bulk carbonate samples (7 from Serrucho creek, 16 from El Plomo creek, 9 from La Vaina and 22 from Potimalal river). Stable isotope analyses were carried out following the usual techniques (McCrea, 1950 and later modifications) and measured in a Delta S Finnigan Mat triple-collector mass spectrometer. The isotopic composition is reported as deviation per mil ($\delta‰$) relative to the V-PDB standard. The analytical error is 0.1‰ ($\pm 2\sigma$) for both $\delta^{13}C$ and $\delta^{18}O$. Sr, Mn and Fe concentrations were determined by wavelength dispersive X-ray fluorescence spectrometry (Philips PW1410). International standards NBS-1b, NIST-1c, NIST-88b, JLs-1 and JDo-1 were used as reference materials. Strontium isotopes were analyzed at the Centro de Geociencias, Universidad Federal do Pará, Brazil. $^{87}Sr/^{86}Sr$ ratios were determined (3 samples from El Plomo creek, 2 from La Vaina and 6 from Potimalal river) with a thermo-ionization multicollector mass spectrometer Finnigan MAT-262. The $^{87}Sr/^{86}Sr$ ratio of the standard NBS-987 during operating conditions was 0.71023 ± 0.000015 (2δ).

4. Facies analysis

4.1. Facies/microfacies associations and depositional setting

A detailed analysis of facies and microfacies of the Calabozo Formation, as well as the study of their vertical and regional distribution (Fig. 3), allowed to define the subenvironments and

characterize this eocallovian homoclinal ramp development. Subenvironments range from proximal outer ramp to mid ramp and inner ramp composed by peritidal, protected lagoons and bar complexes in a context of a highstand stage. The sequence reveals a significant shallowing trend culminating in the progressive isolation of the basin, which provided suitable hypersalinity conditions for the development of evaporitic facies of Tábanos Formation.

The terminology used was proposed by Wright and Burchette (1996), who defined the outer ramp as the zone below normal storm wave base that extends to the basin floor, the mid ramp is located between the storm wave base and the fair weather wave base, and the inner ramp is that zone above fair weather wave base including high energy environments (shoreface and beach) as well as subtidal back shoal deposits and peritidal and supratidal environments. Field characterization of the facies layers was complemented with the petrographic description of thin sections.

This section integrates information from former studies carried out by Cabaleri et al. (2003, 2007) and Armella et al. (2005a, b) with additional analysis.

4.1.1. Outer ramp

This subenvironment is only represented in the outcrops of Potimalal river (Fig. 3) by 3.50 m thick abundant shale levels interbedded with thin packstone and mudstone beds recording small sea level fluctuations. Facies and microfacies association corresponds to proximal outer ramp deposits, and represents the deepest deposits of the Calabozo Formation sequence. Table 1 provides a summary of facies and microfacies analyzed.

4.1.1.1. Proximal outer ramp facies/microfacies (Potimalal river section).

P1 – Bio-siliciclastic packstone. It constitutes the base of the Calabozo Formation profile in Potimalal river. It includes 0.25 m of black shales covered by a bioclastic level (0.05 m) and three beds (0.20–0.40 m) with erosive base and thin shale interbeddings. The contents of unbroken and silicificated bivalves (*Pholadomya* and *Ostrea*) increases in the upper bed. Components are poorly sorted and isooriented micrite intraclasts parallel to stratification (1 × 0.3 cm) have been identified. The microfacies is mainly composed of fragmented bioclasts (20–30%) including bivalve remains (*Pholadomya* and *Ostrea*), echinoderms, brachiopods, dasycladacean algae and scarce bryozoans (Fig. 4B). Lower amounts of siliciclasts (10–15%),

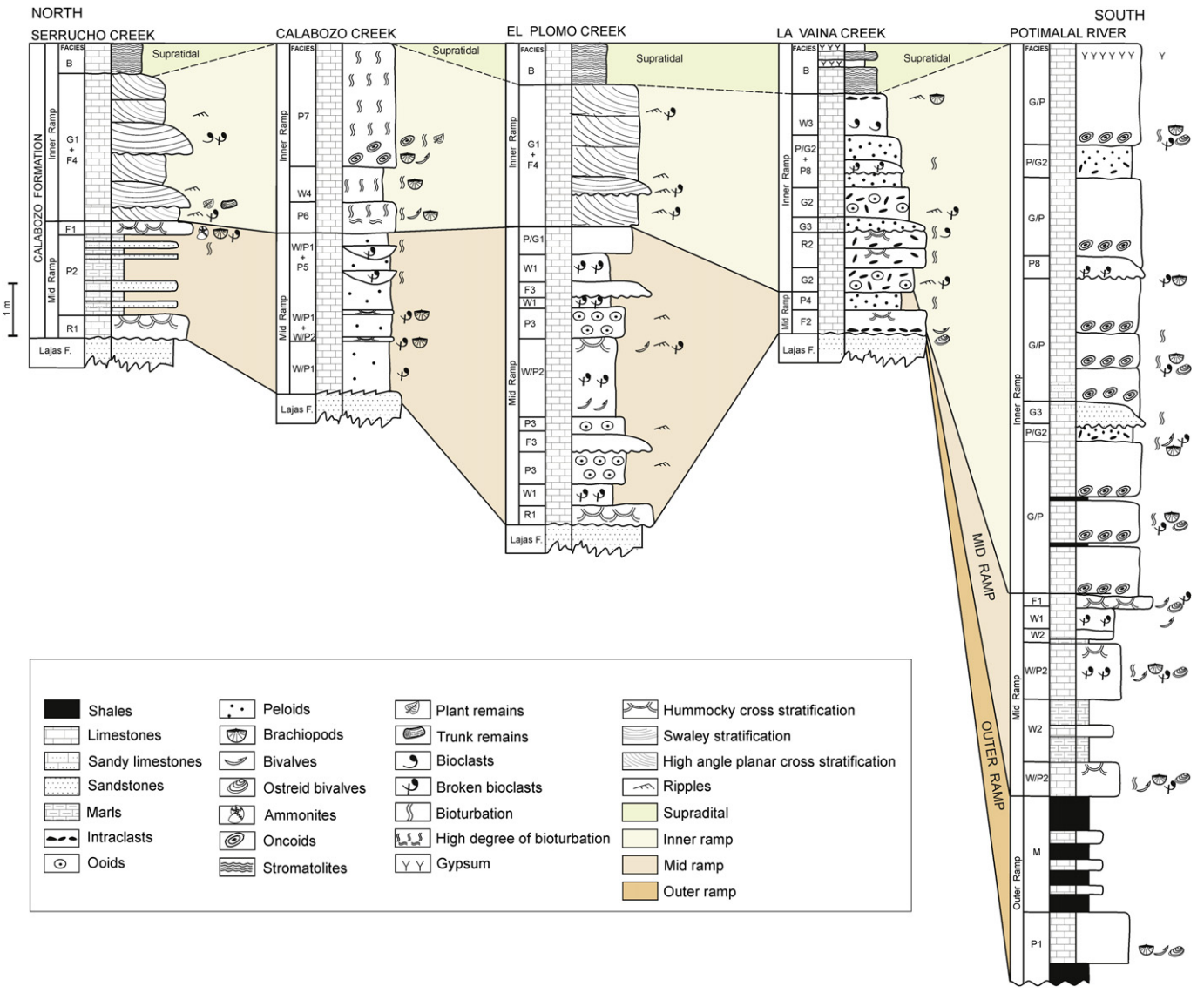

Fig. 3. Columnar sections from studied localities. The panel illustrates the vertical and regional distribution of the facies associations of outer, mid and inner ramp subenvironments. The horizontal distances between the outcrop areas are not to scale.

Table 1
Outer ramp facies/microfacies synthesis.

Facies code	Lithology	Facies associations	Occurrence	Components	Sedimentary structures and fabric	Environmental interpretation
M	**Mudstone** Alternating with black shales		Potimalal river	*Grains*: intraclasts, calcisphers, siliciclasts and bioclasts. *Matrix*: grumous and peloidal micrite	Mud supported	Proximal outer ramp Low energy conditions
P1	**Bio-siliciclastic packstone** Alternating with black shales		Potimalal river	*Grains*: bioclasts, siliciclasts, calcisphers, intraclasts peloids and faecal pellets. *Matrix*: peloidal micrite	Poorly sorted grains. Occasionally oriented particles.	Proximal outer ramp Sporadic bottom currents

sparite calcisphers (10%), micrite intraclasts (5–10%) and fecal pellets (5%) were also identified. In some levels particles are aligned. Matrix is composed of peloidal micrite and scarce microsparite.

Interpretation: *This moderate energy facies, corresponding to the transition between Lajas and Calabozo formations, is coincident with the change in sedimentation style from siliciclastic to carbonatic. Carbonate deposits were originated under well oxygenated water conditions and scarce detrital input, suitable for the development of benthos. The presence of occasionally oriented particles and bioclasts suggests an influence of sporadic bottom currents*.

M* – *Massive mudstone. This facies is 2.10 m thick and is characterized by the interbedding of black shales and mudstone levels (0.05 m thick). They are composed of grumous and peloidal micrite with scarce fine sparite cement. Scattered particles (<10%) corresponding to micrite intraclasts with clay material, sparite calcisphers, very fine siliciclasts and bioclasts were observed in upper levels. Bioclasts consist of bivalve remains, echinoderms, bryozoans and gastropods filled with micrite and clay material (Fig. 4A). Scattered idiomorphic crystals of iron oxide (1%) were identified.

Interpretation: *Fine material sedimentation by suspension or decantation, in low energy (subtidal) conditions forming undisturbed substrates*.

4.1.2. Mid ramp

Micrite muds containing abundant nutrients, accumulated in a subtidal to intertidal environment. The mid ramp subenvironment is characterized by an increase in biota and fragmented bioclast contents. The presence of benthonic fauna including bivalves, brachiopods, gastropods and echinoderms, as well as dasycladacean algae and frequently bioturbated substrates, suggest clear water conditions in the photic area, regular salinity and oxygen content. Stormy weather waves produced episodes of disturbance on the substrate with the consequent reworking and redistribution of particles and bioclasts. The mid ramp subenvironment is represented in the following sections: Serrucho creek (2.60 m thick), Calabozo creek (3 m), El Plomo creek displaying a maximum development (6 m), La Vaina creek and in Potimalal river (3.80 m). In La Vaina section mid ramp facies are transitional to inner ramp subenvironment. The major terrigenous input was recorded at the north of the ramp in Serrucho creek and Calabozo creek localities, decreasing considerably towards the south. A summary of facies and microfacies characteristics of mid ramp environments are shown in Table 2.

4.1.2.1. Moderate to low energy facies/microfacies (Serrucho creek, Calabozo creek, El Plomo creek and Potimalal river sections) (Fig. 3).

W1* – *Pelointraclastic wackestone. This facies was identified in El Plomo creek and Potimalal river sections and is characterized by tabular beds from 0.20 m to 0.40 m thick. Deposits of fragmented shells locally oriented and micrite intraclasts on bed surfaces are characteristic of this facies. In lower levels of the Potimalal river section bivalve fauna in life position was observed. Pelointraclastic wackestone beds in El Plomo creek locality are associated to floatstone lenticular bodies (**F3**). This microfacies (Fig. 5A and B) is characterized by high contents of massive micrite peloids and fecal pellets (15–20%), micrite intraclasts (5–15%), and micrite ooids (10%). Bioclasts (5–15%) consist of bivalves (*Pholadomya* and *Ostrea*), brachiopods, gastropods, echinoderms, coral, poorly preserved foraminifers and dasycladacean algae. Calcispheres and subangular siliciclast crystals were observed in lower contents. Matrix is peloidal micrite with very fine sparite cement.

Interpretation: *Biota and particle association implies calm shallow water conditions in low energy subtidal environment with a soft substrate dissected by channels (**F3**). Tractive bottom currents originated isooriented intraclasts and bioclasts deposits.*

***W2* – *Bioclastic wackestone* (*Fig. 5C*)**. This facies only outcrops in the Potimalal river section and is composed of thin layers (15 cm–20 cm thick) interbedded with marly shale levels. Bioclasts (15%) are highly fragmented and gathered into groups forming local accumulations. Bivalve shell remains, echinoderms, gastropods and undefined foraminifers are dominant. Scarce sparite intraclasts (5%), calcisphers and scattered siliciclasts were observed. Matrix is peloidal micrite with very fine siliciclasts.

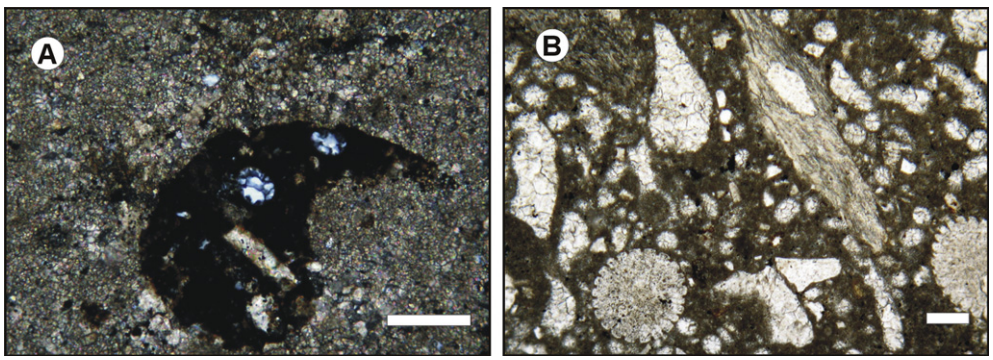

Fig. 4. Photomicrographs of outer ramp microfacies. Scale bars: 200 μm. A: **Massive mudstone** (**M**), clay filled bioclasts in a grumous micrite matrix, with sparite cement. Sample CAPO6. B: **Bio-siliciclastic packstone** (**P1**), Bivalve shell remains (*Ostrea*) and echinoderm spines, sparite calcispheres, micrite intraclasts and siliciclasts in a peloidal micrite matrix. Sample CAPO4.

Table 2
Mid ramp facies/microfacies synthesis.

Facies code	Lithology	Facies associations	Occurrence	Components	Sedimentary structures and fabric	Environmental interpretation
W1	**Pelointraclastic wackestone**	F4 (channels)	El Plomo creek Potimalal river	*Grains*: peloids and faecal pellets, intraclasts, ooids, bioclasts. *Matrix*: peloidal micrite	Occasionally orientated particles. Bivalves in life position in the lower levels of Potimalal river.	Subtidal substrate affected by bottom currents
W2	**Bioclastic wackestone** alternating with marly shales		Potimalal river	*Grains*: bioclasts, sparite intraclasts. *Matrix*: peloidal micrite	Local concentration of bioclast remains	Subtidal substrate affected by bad weather wave base.
W/P1	**Siliciclastic intrapeloidal wackestone/packstone**	W/P2 (storm deposits) P5 (channels)	Calabozo creek	*Grains*: siliciclasts, intraclasts, black pebbles, peloids, ooids and bioclasts. *Matrix*: grumous and peloidal micrite	Ripples	Subtidal substrate affected by sporadic bad weather waves
P2	**Sandy packstone with marls interbedded**		Serrucho creek	*Grains*: siliciclasts, intraclasts. *Matrix*: grumous and peloidal micrite	Well sorted and oriented particles. Bioturbation.	Subtidal deposits with continental input.
W/P2	**Biointraclastic wackestone/packstone**	W/P1 (subtidal deposits) Marls levels	Calabozo and El Plomo creeks, Potimalal river	*Grains*: bioclasts, intraclasts, ooids and peloids. *Matrix*: peloidal micrite with sparite cement	Hummocky cross-stratification Amalgamated beds. Ripples.	Storm deposits
P3	**Oobioclastic packstone**	F4 (channels)	El Plomo creek	*Grains*: mainly cortoids: ooids, bioclasts and intraclasts. *Matrix*: grumous and peloidal micrite, sparite cement.	Ripples Amalgamated beds. Well sorted and grain supported	Wave influenced deposits
P4	**Peloidal packstone**		La Vaina creek	*Grains*: peloids, bioclasts, intraclasts, black pebbles, plasticlasts. *Matrix*: grumous micrite with sparite cement.	Hummocky cross-stratification Very fragmented particles	Storm deposits
P/G1	**Intraclastic packstone/grainstone**	G1 (inner ramp shoals)	El Plomo creek	*Grains*: intraclasts with variable composition, mostly from other microfacies. Bioclasts and ooids. *Matrix*: microsparite and sparite blocky cement	Bioturbation	Seaward shoal deposits
R1	**Sandy intraclastic rudstone**		Serrucho and El Plomo creeks	*Grains*: siliciclasts, lithoclasts (mainly volcanic origin), intraclasts. *Matrix*: intrasiliciclastic packstone	Hummocky cross-stratification. Grain supported. Oriented particles	High energy event
F1	**Skeletal floatstone with skeletal packstone matrix**		Serrucho creek Potimalal river	*Grains*: bioclasts, (bivalves, brachiopods, ammonites). *Matrix*: skeletal packstone	Hummocky cross-stratification Matrix supported	Storm deposits
F2	**Skeletal floatstone with peloidal wackestone matrix**	Erosive contact over Lajas Formation	La Vaina creek	*Grains*: bioclasts and scarce intraclasts. *Matrix*: peloidal wackestone	Intraclastic lag Hummocky cross-stratification. Bivalves in life position at the bottom. Matrix supported	High energy event
P5	**Biopeloidal packstone**	W/P1 (subtidal deposits)	Calabozo creek	*Grains*: bioclasts, peloids, intraclasts. *Matrix*: grumous and peloidal micrite. Scarce sparite cement	Thin lenticular levels. Mud supported	Ephemeral channels
F3	**Oobiointraclastic floatstone**	P3 W1	El Plomo creek	*Grains*: ooids, bioclasts, intraclasts, siliciclasts. *Matrix*: peloidal micrite and esparite blocky cement	Lenticular levels with erosive contact. Poorly sorted particles	Channels

Interpretation: *Substrates disturbed by bad weather waves. These waves produced local turbulence that broke and concentrated bioclastic remains.*

W/P1 – Siliciclastic intrapeloidal wackestone/packstone. This facies is recognized at the base of the Calabozo creek section and is associated to lenticular levels (**W/P2** and **P4**). Beds range from 0.30 m to 0.50 m thick and show ripples on the strata surfaces. Thin sections (Fig. 5D) studied revealed angular siliciclasts (15%), micrite intraclasts (10%), some cortoids, black pebbles (5%), peloids (5%) and ooids (1%). Bioclasts (3%) are represented by brachiopod fragments (rhynchonellids), bivalves and gastropods. Matrix is made up of grumous and peloidal micrite with scattered iron oxide nodules.

Interpretation: *Particle association and the presence of ripples suggest depositional conditions in a subtidal environment where the substrate was carved by thin channels and occasionally affected by bad weather waves (**W/P2**).*

P2 – Sandy packstone with interbedded marls. This 1.40 m thick facies outcrops at the lower part of the Serrucho creek section. It is defined by thin interbedded sandy limestone levels with ripples and marls. At the lower levels particles are aligned and at the upper levels, bioturbation with *Ophiomorpha* type traces was observed. The microfacies corresponds to packstone containing abundant detrital material (Fig. 5E). Particles are well sorted, very fine (30–50%) and medium fine size sand (5–10%) They are composed of angular siliciclasts (quartz, feldspar and mica) and lithoclasts, micrite intraclasts (2%) and scarce broken ooids (0.5%). Bioclasts are represented by algae filaments and bivalve remains. Matrix is grumous peloidal micrite.

Interpretation: *Sedimentation of fine material by decantation in a subtidal environment, disturbed by currents with detrital material input from the continent.*

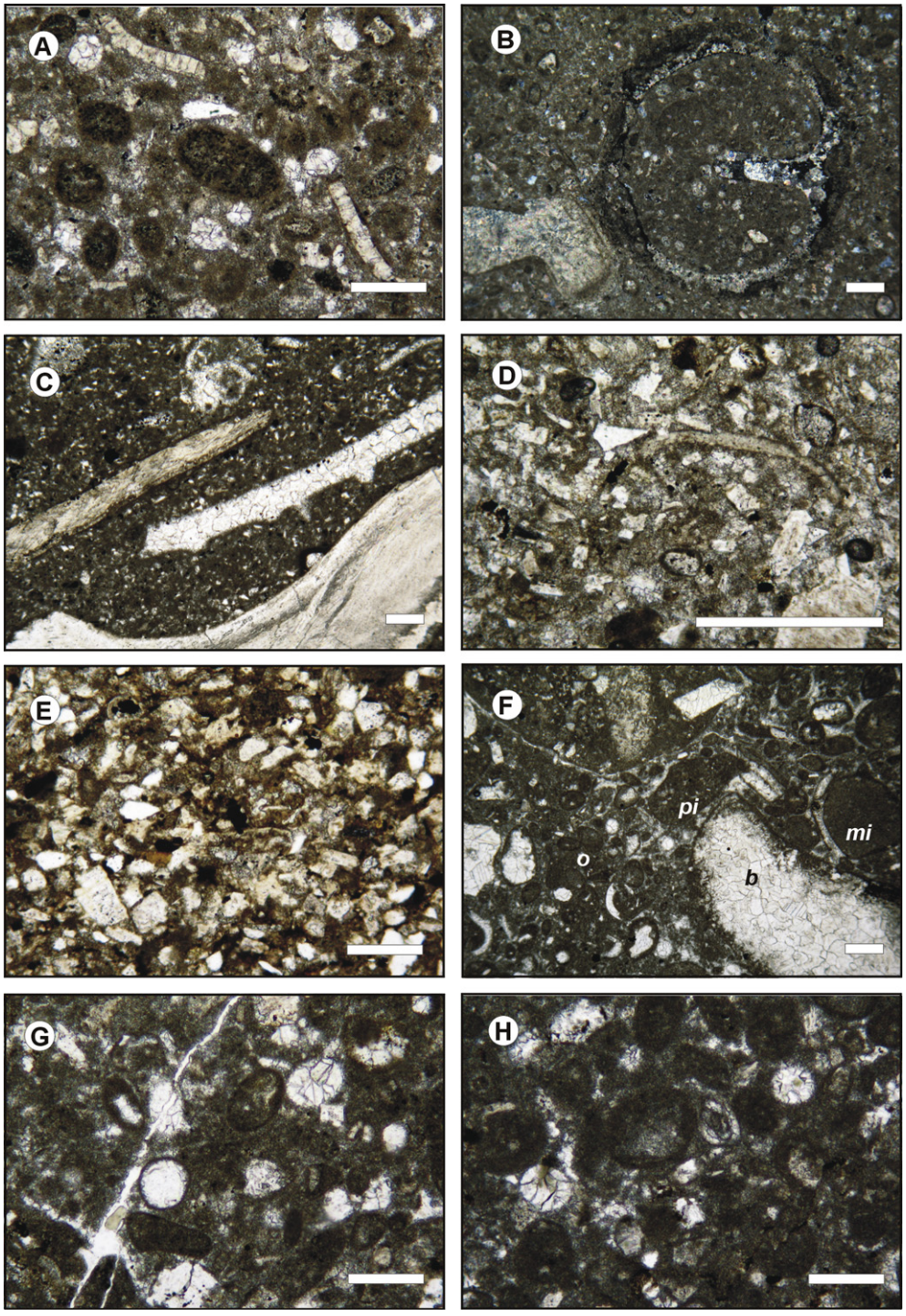

Fig. 5. Photomicrographs of mid ramp microfacies. Scale bars: 200 μm. A: **Pelointraclastic wackestone** (**W1**), micrite intraclasts with scattered iron oxides, micrite peloids and bioclasts in a peloidal micrite matrix with sparite cement. Sample CAPO11. B: **Pelointraclastic wackestone** (**W1**), gastropod section, micrite peloids, micrite intraclasts, sparite calcispheres, siliciclasts and peloidal micrite matrix. Sample CAPO11. C: **Bioclastic wackestone** (**W2**), bivalve shell remains and gastropod section in a peloidal micrite matrix. Sample CAPO8. D: **Siliciclastic intrapeloidal wackestone/packstone** (**W/P1**), angular siliciclasts, bioclasts, ooids and iron oxide crystals scattered in the peloidal grumous micrite matrix. Sample CAC1. E: **Sandy packstone** (**P2**), well sorted angular siliciclasts, micrite intraclasts and peloidal grumous micrite matrix. Sample ASC3. F: **Biointraclastic wackestone/packstone** (**W/P2**), bioclasts with endolithic algae cover (b), micritic intraclasts (mi), intraclasts composed of peloidal micrite (pi), ooids (o), siliciclasts and peloidal micrite matrix with sparite cement. Sample CAP10T. G: **Oobioclastic packstone** (**P3**), micrite ooids and sparite nucleus ooids, micrite intraclasts in a grumous matrix with sparite cement. Sample CAP6. H: **Peloidal packstone** (**P4**), micrite peloids, micrite intraclasts, foraminifer section, sparite calcispheres in a peloidal micrite matrix. Sample CAVA18T.

4.1.2.2. High energy facies/microfacies (Serrucho creek, Calabozo creek, El Plomo creek and Potimalal river sections) (Fig. 3).

W/P2 – Biointraclastic wackestone/packstone (Fig. 5F). In El Plomo creek and Potimalal river sections, this facies is represented by amalgamated beds approximately 0.60 m thick. Benthos is mainly composed of bivalves (*Weyla*, *Ostrea* and *Pholadomya*) in life position at the base, and scrambled and broken bivalve debris in the upper levels. Unlike other locations, in Calabozo creek this facies outcrops in very thin levels (0.15 m), containing mainly brachiopods (rhynchonellids) fauna. Bioturbation, ripples, and hummocky

cross-stratification are recognized at the top of the beds. The microfacies is characterized by high contents of bioclasts (20% in Calabozo creek and El Plomo creek section, 50% in Potimalal river). Skeletal grains include bivalve remains, brachipods (mainly rhynchonellids), gastropods, echinoderms, bryozoans, foraminifers and fish scales associated with dasycladacean algae remains and *Girvanella*. Minor micrite intraclasts (5–10%), ooides (1–5%), peloids (1–5%) and scarce subangular siliciclasts (1%) were recognized. Matrix is peloidal micrite with scarce sparite cement.

Interpretation: *The erosion surfaces between amalgamated beds, the ripples and hummocky cross-stratification in association with bivalves in life position and broken bioclasts, indicate storm episodes disturbing subtidal shallow deposits colonized by benthonic organisms.*

P3 – Oobioclastic packstone (Fig. 5G). This facies was identified in El Plomo creek section and it is characterized by amalgamated beds of approximately 0.20 m–1.50 m thick, with wave ripples in the upper levels. In the lower levels, this facies is dissected by lenticular bodies corresponding to channel deposits (**F3**). Particles are well sorted, reworked and covered by micritic envelopes. Tangential micrite and esparite ooids predominate, some of them containing bioclastic or sparite nucleus. Bioclast contents increase in the upper levels (20–45%). Organic remains correspond to fragmented echinoderms, gastropods, bryozoans, bivalves, foraminifers, coral, amonites, fish scales and dasycladacean algae. Intraclasts (5–15%) and faecal pellets (5%) are also commonly observed. Some particles presented iron oxide rims. Matrix is grumous micrite with sparite cement.

Interpretation: *Amalgamated beds and wave ripples suggest a substrate affected by fair weather waves in shallow areas. Abundant ooids indicate bars proximity and input from the inner ramp subenvironment facies by channels.*

P4 – Peloidal packstone (Fig. 5H). This facies outcrops in La Vaina creek section and corresponds to thin (0.10 m–0.20 m) tabular levels, with erosive surfaces and slightly noticeable hummocky cross-stratification In thin section the microfacies is characterized by very fragmented particles, mainly micrite peloids (30%). It is also composed of lower quantities of bioclasts (15%) corresponding to bivalve, brachiopod, foraminifers, algae remains, superficial and tangential ooids (10–20%) with sparite nucleus, micrite intraclasts (10–15%) including black pebbles, intraclasts from other microfacies, plasticlasts, and scarce siliciclasts (1%). Matrix is grumous peloidal micrite with granular sparite cement.

Interpretation: *Deposits from shallow subtidal environment influenced by storms. Particle association indicates inputs from subtidal and shore areas.*

P/G1 – Intraclastic packstone/grainstone. A 0.50 m thick bed with *Thalassinoid*, *Planolites* and *Teichichnus* bioturbation was recognized in El Plomo creek locality. The microfacies (Fig. 6A) includes mainly well rounded micrite intraclasts (30%), mostly constituted by remains from other microfacies, and fragmented bivalve bioclasts (15%), echinoderms, foraminifers, fish scales and dasycladacean algae. Ooids (15%) are micritic, radial or containing bioclast or intraclast nucleus, similar to those formed in the inner ramp subenvironment. Matrix is microesparite, with sparite blocky cement.

Interpretation: *Intraclasts composed of remains from other microfacies, ooids and reworked bioclasts indicate that grainstone shoals influenced by continuous wave movement and tidal action are the main material source. According to Pemberton et al. (1992), ichnofacies association indicates softground substrate in a well oxygened shallow intertidal/subtidal environment.*

R1 – Sandy intraclastic rudstone. This facies represents the base level in the Serrucho creek and El Plomo creek sections. In the latter locality, it lies in erosive contact on the siliciclastic facies of Lajas Formation. It is represented by a 0.50 m thick tabular bed with hummocky cross-stratification. Texture is clast supported with normal gradation, dominant coarse grain-size clast types include siliciclasts (45%) and clasts of volcanic rocks, 1.5 cm–20 cm in size. Minor micrite intraclasts (15–30%), 2 cm–10 cm in size, and bivalve remains are also recognized. Micrite intraclasts are dominant in Serrucho creek, while in El Plomo creek siliciclasts are widespread. Particles are reworked, frequently oriented and imbricated. Rudstone matrix is an intrasiliciclastic packstone (Fig. 6B) composed of micrite intraclasts (10–15%), some with algal micrite covers, siliciclasts (10–15%), tangential and radial ooides (5–20%) and bioclasts (5–10%), represented by bivalve fragments, cephalopods and dasycladacean algae. Packstone matrix is grumous micrite with sparite blocky cement.

Interpretation: *Hummocky cross-stratification, particle isoorientation and the association of reworked extrabasinal (siliciclasts and coarse lithoclasts) and marine components, suggest a siliciclastic substrate disturbed and eroded by a high energy event. This facies represents the marine ingression, which affected the marginal marine/deltaic plain facies of Lajas Formation. This facies indicates the beginning of the carbonatic sedimentation regime, distinctive of the Calabozo Formation (Cabaleri et al., 2003).*

F1 – Bioclastic floatstone with skeletal packstone matrix. This facies is present in the upper level of the mid ramp sequence at Serrucho creek and Potimalal river sections. It consists of approximately 0.20 cm thick beds with erosive base and hummocky cross-stratification. It is characterized by high contents of fragmented bioclasts (20%). At Serrucho creek, brachiopod remains and scattered unbroken amonites 20 cm in diameter are abundant in the packstone matrix, while at Potimalal creek, bivalve remains (*Pholadomya* sp. and *Ostrea*) are predominantly present. Particles of the microfacies (Fig. 6C) are very fragmented. Bioclasts (20%) include bivalve remains, gastropods, brachiopods and possibly fish scales. Micrite, massive or radial tangential ooids (15%) are increasingly present in Potimalal river section. Lower quantities of faecal pellets, peloidal intraclasts and siliciclasts have been observed. Matrix is grumous micrite and pore spaces are filled with granular sparite.

Interpretation: *Deposits were accumulated in subtidal/intertidal conditions and were disturbed by storm events. Higher contents of ooids and bivalve remains in the south of the ramp (Potimalal river) could indicate increased material input from shoal and shore facies compared to the Serrucho creek section.*

F2 – Bioclastic floatstone with peloidal wackestone matrix. This facies overlies in erosive contact with the silicicclastic facies of Lajas Formation in La Vaina creek section. It is represented by a 0.30 m thick bed with hummocky cross-stratification and an intraclastic level at the base. Bivalves (*Pholadomya* and *Ostrea*) in life position were observed in lower levels, while removed bioclasts (15%) and scarce micrite intraclasts (5%) 1–2 cm in diameter, were identified in the rest of the bed. Floatstone matrix is peloidal wackestone (Fig. 6D) composed of micrite peloids (15–20%), micrite intraclasts (15%) occasionally covered by iron oxides, black pebbles showing evidence of subaerial exposure, ooides (10%) and faecal pellets (5%). Bioclasts (10%) include cephalopod fragments, crinoids, algae and fish scales. Matrix is grumous peloidal micrite and microesparite.

Interpretation: *The hummocky cross-stratification, plus the presence of a residual intraclastic level (lag), reflects the influence of a high energy event in the removal and depositation of particles. This event disturbed marginal deltaic facies of Lajas Formation and established shallow subtidal conditions suitable for benthonic organism development.*

4.1.2.3. Channel facies/microfacies (Calabozo creek and El Plomo creek sections).

P5 – Biopeloidal packstone (Fig. 6E). Thin (0.20–0.10 m) lenticular levels appear in the Calabozo creek section associated to

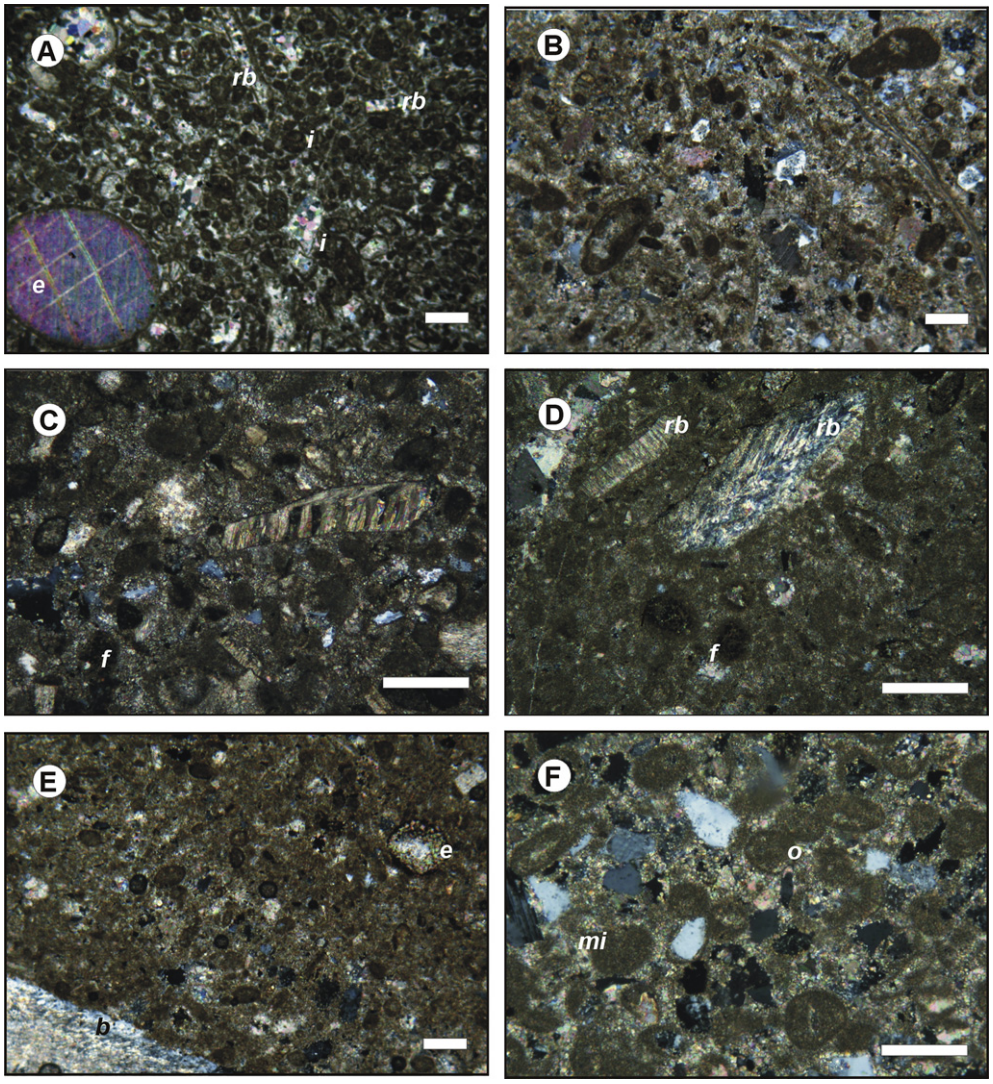

Fig. 6. Photomicrographs of mid ramp microfacies. Scale bars: 200 μm. A: **Intraclastic packstone/grainstone** (**P/G1**), echinoderm plate (e), reworked bioclasts (rb), well rounded intraclasts of micrite and of the other microfacies, ooids and sparite blocky cement. Sample CAP14. B: Thin section of rudstone (**R1**) matrix, **intrasiliciclastic packstone**, angular siliciclasts, micrite intraclasts, micrite ooids, bioclasts, in a grumous micrite matrix with sparite blocky cement. Sample ASC1. C: Thin section of floatstone (**F1**) matrix, **skeletal packstone**, brachiopod remains, micrite ooids, peloids, siliciclasts, faecal pellets (f) and grumous micrite matrix with sparite cement. Sample CAPO12. D: Thin section of floatstone (**F2**) matrix, **peloidal wackestone**, reworked bioclasts (rb), peloids, faecal pellets (f), micrite intraclasts, grumous micrite matrix, microesparite and sparite cement. Sample CAVA1. E: **Biopeloidal packstone** (**P5**), bivalve shell remains (b), echinoderm remains (e), peloids, siliciclasts and peloidal micrite matrix. Sample CAC5. F: **Oobiointraclastic floatstone** (**F3**), micrite ooids (o), micrite intraclasts (mi), angular siliciclasts and sparite blocky cement. Sample CAP8.

W/P1 facies. They are composed of very fragmented bioclasts (10%) corresponding to bivalve remains, ostracods, echinodems, foraminifers and dasycladacean algae; micrite peloids (10%), scarce micrite intraclasts (5%) and black pebbles. Matrix is grumous peloidal micrite, affected by bioturbation with scarce sparite cement.

Interpretation: *The geometry and low thickness of the bed as well as the fragmentation degree of particles suggests ephemeral channeled flows that migrated over unconsolidated substrate, and supplied material input from coastal areas.*

F3 – Oobiointraclastic floatstone. This facies corresponds to lenticular bodies (0.70–3 m long and 0.40 m thick) which outcrop in El Plomo creek section and are in erosive contact with **P3** and **W1** facies. Particles are normally graded, fragmented and poorly sorted. Microfacies (Fig. 6F) is constituted by superficial and radial micrite ooids (20%), very fragmented bioclasts (20%), well rounded micrite intraclasts (15%), some covered by thin micrite envelopes, and angular siliciclasts (15%). Matrix is made up of micrite and pores are filled with sparite blocky cement. Bioturbation borings were observed.

Interpretation: *Lenticular bodies with erosive base represent channel deposits that dissected the substrate (**P3** and **W1** facies). Particle association, their fragmentation degree and normal grading suggest shallow discharge flows possibly due to temporary increase of water input to the ramp. Sediments were transported from coastal areas and shoals to mid ramp facies.*

4.1.3. Inner ramp

The inner ramp subenvironment is well represented (Fig. 3) in the mid and upper section of the Calabozo Formation sequence and outcrops in all the studied localities: Serrucho creek (3.40 m thick), Calabozo creek (4.10 m), El Plomo creek (3.45 m), La Vaina creek (4.65 m) and Potimalal river (10.40 m). In order to offer a clear description, this subenvironment was divided into five facies and microfacies associations involving tidal flat facies with ooidal shoals dissected by tidal channels, and protected environment

facies (Table 3). Environmental conditions in peritidal facies were suitable for the development of biota composed of bivalves (*Pholadomya*), gastropods (nerineids), echinoderms, brachiopods, bryozoans, dasycladacean algae, halimedacean, cyanobacteria and scarce foraminifers. Vertical and subhorizontal perforations, corresponding to Ichnofacies of *Ophiomorfha*, *Skoliltos*, *Thalassinoide* and *Glossitfungites* were recognized. Calabozo creek beds are characterized by intense bioturbation with a high density of cylindric to subcylindric subhorizontal burrows carved by worms.

4.1.3.1. Peritidal facies/microfacies (Serrucho creek, El Plomo creek, La Vaina creek and Potimalal river sections) (Fig. 3).

B – Stromatolite boundstone. In El Plomo creek, La Vaina creek and Potimalal river sections, stratiform stromatolites have been identified in the upper levels of the unit, while in Serrucho creek section, scattered stromatolite fragments were recognized. They are displayed in 0.10 m–0.30 m thick layers (Fig. 7A), constituted by sets of thin micrite laminae (1–2 mm), with fenestral fabric and interstitial gypsum. Stromatoids are discontinued, crenulated in

Table 3
Inner ramp facies/microfacies synthesis.

Facies code	Lithology	Facies associations	Occurrence	Components	Sedimentary structures and fabric	Environmental interpretation
B	**Stromatolite boundstone**		Serrucho, El Plomo and La Vaina creeks, Potimalal river	Sets of peloidal micrite stromatoids with fenestral fabric and gypsum. Stromatoids r eplaced by silica in La Vaina creek	Stratiform stromatolites. Mudcracks	Supratidal
W3	**Biointraclastic wackestone**		La Vaina creek	*Grains*: Bioclasts (with endolithic algae cover), intraclasts, ooids and rare siliciclasts. *Matrix*: peloidal micrite with scarce sparite cement.	Bivalves in life position and fragmented remains. Ripples. Poor sorted particles.	Tidal flat
P/G2	**Intraoobioclastic Packstone and grainstone**	P8 and G3 (channels) G2 and G/P (shoals and bars)	La Vaina creek Potimalal river	*Grains*: intraclasts (micritic and ooids composed), concentric and radial ooids, bioclasts. *Matrix*: grumous micrite and sparite blocky cement	Normally graded beds. Bioturbation. Fenestral micrite fabric. Gypsum molds in the top level of Potimalal river Poor sorted particles	Tidal flat deposits back shoals
W4	**Peloidal wackestone with intense bioturbation**	Alternating with sandy wackestone/mudstone beds in the upper levels.	Calabozo creek	*Grains*: peloids, intraclasts, faecal pellets, ooids and scarce bioclasts and siliciclasts. *Matrix*: peloidal micrite, burrows filled by microsparite/sparite cement.	Intense bioturbation Low diversity of fauna. Mud supported	Protected environment (lagoon) with continental input and ephemeral ponds
P6	**Bioclastic packstone with intense bioturbation**		Calabozo creek	*Grains*: Mainly bioclast, peloids, intraclasts, ooids rare black pebbles and faecal pellets. *Matrix*: peloidal micrite with organic matter	Intense worm bioturbation	Protected environment (lagoon)
P7	**Bioturbated peloidal packstone**	W4 (lagoon)	Calabozo creek	*Grains*: peloids, faecal pellets, bioclasts, rare oncoids and ooids. *Matrix*: grumous and peloidal micrite with bioturbation.	Intense worm bioturbation. Grain supported	Tidal flat protected environment with continental input
G1	**Intrabiooidal grainstone**	North ramp bar complex F5 (channels)	Serrucho and El Plomo creeks	*Grains*: micritic and composed intraclasts, bioclasts, concentric ooids and oncoids. *Cement*: sparite blocky	Amalgamated beds. Cross-stratification. Ripples Bioturbation	Shoal/bars affected by fair weather waves and currents.
F4	Intrabioclastic floatstone	North ramp bar complex G1 (shoal/bars)	Serrucho and El Plomo creeks	*Grains*: intraclasts, bioclasts (with trunks remains). *Matrix*: skeletal wackestone/packstone	Lenticular beds. Swaley cross-stratification. Ripples. Poor sorted particles.	**Channels** with shoals and continental input
G/P	**Oobioclastic grainstones and packstones**	South ramp bar complex: P/G2 (tidal flat) G3 and P8 (channels)	Potimalal river	*Grains*: concentric ooids, bioclasts, siliciclasts and intraclasts (micritic and ooids composed). *Matrix*: sparitic blocky cement and peloidal micrite.	Amalgamated beds. Basal levels with oriented particles Bioturbation. Mudcracks and gypsum	Bars affected by fair weather waves
G2	**Intraoobioclastic grainstone**	South ramp bar complex	La Vaina creek	*Grains*: intraclasts, ooids, bioclasts, scarce siliciclasts, peloids and ooids. *Cement*: sparite	Amalgamated beds Bioturbation Grain supported with well sorted particles	Shoals
P8	**Biooidal packstone**	South ramp bar complex: P/G2 (tidal flat) G/P (bars)	La Vaina creek Potimalal river	*Grains*: bioclasts, ooids and intraclasts. *Matrix*: grumous and peloidal micrite. Sparite and scarce radial silica cement.	Lenticular levels Bioclasts with endolithic algae borings	Tidal channels with tidal flat and bars input
G3	**Oosiliciclastic grainstone**	South ramp bar complex: F6 (storm deposits), G2 (shoals) P/G2 (tidal flat)	La Vaina creek Potimalal river	*Grains*: cortoids particles, concentric and radial ooids, siliciclasts, composed intraclasts and bioclasts. *Cement*: sparite	Lenticular beds Swaley cross-stratification and horizontal lamination in the top Well sorted particles.	Channels with shoals and continental input
R2	**Intraclastic rudstone**	G2 (shoals) G3 (channels)	La Vaina creek	*Grains*: intraclasts, plasticlasts, bioclasts. *Matrix*: bioclastic wackestone/packstone	Amalgamated beds. Hummocky c ross-stratification Grain supported.	Back shoal deposits affected by bad weather waves

profile and show horizontal attitude. Mudcracks are frequent. Stromactatis increase up-section within the facies. Under microscopic study, microbialitic lamination is defined by alternation of microsparite stromatoids with fenestral texture and peloidal micrite stromatoids. In stromatolites from La Vaina creek, stromatoids are replaced by microcrystalline radial silica with equigranular silica cement.

Interpretation: *The development of microbial communities adapted to higher evaporation conditions, and increased salinity in marginal waters originated stromatolite levels with gypsum.*

W3 – Biointraclastic wackestone. This facies represents the upper levels of the Calabozo Formation sequence in La Vaina creek profile. It is characterized by a 0.70 m thick tabular bed containing bivalves (*Pholadomya* and *Ostrea*) in life position or in transported fragments. This facies culminates with a thin level with ripples and well rounded micrite intraclasts 2 cm in diameter. The microfacies mainly presents bioclasts (15%) often covered with endolithic algae (Fig. 7B). Bioclasts include bivalve fragments, braquiopods, echinoderm remains and algae detritus. Lower amounts (12%) of intraclasts, micrite peloids, micrite ooids and scarce siliciclasts (3%) have been identified. Matrix is made up of peloidal micrite with low sparite contents. Particles are reworked and poorly sorted.

Interpretation: *Reworked particles with microborings by endolithic algae action and occasional iron oxide rims, in addition to the presence of ripples, indicate tidal flat sedimentation under moderate energy conditions. The environment was suitable for bivalve development in a soft substrate.*

P/G2 – Intraoobioclastic packstone/grainstone (Fig. 7C). This facies is mainly characterized by normally graded beds of 20 m–0.60 m thick, some of which turn to massive structure. Borings by *Glossifungite* Ichnofacies are frequent. This facies, outcropping in the southern of the ramp is dissected by lenticular bodies (**P8** in La Vaina creek and **G3** in Potimalal river), and lies in erosive contact with the ooidal bodies (**G2** and **G/P**). In Potimalal river section,

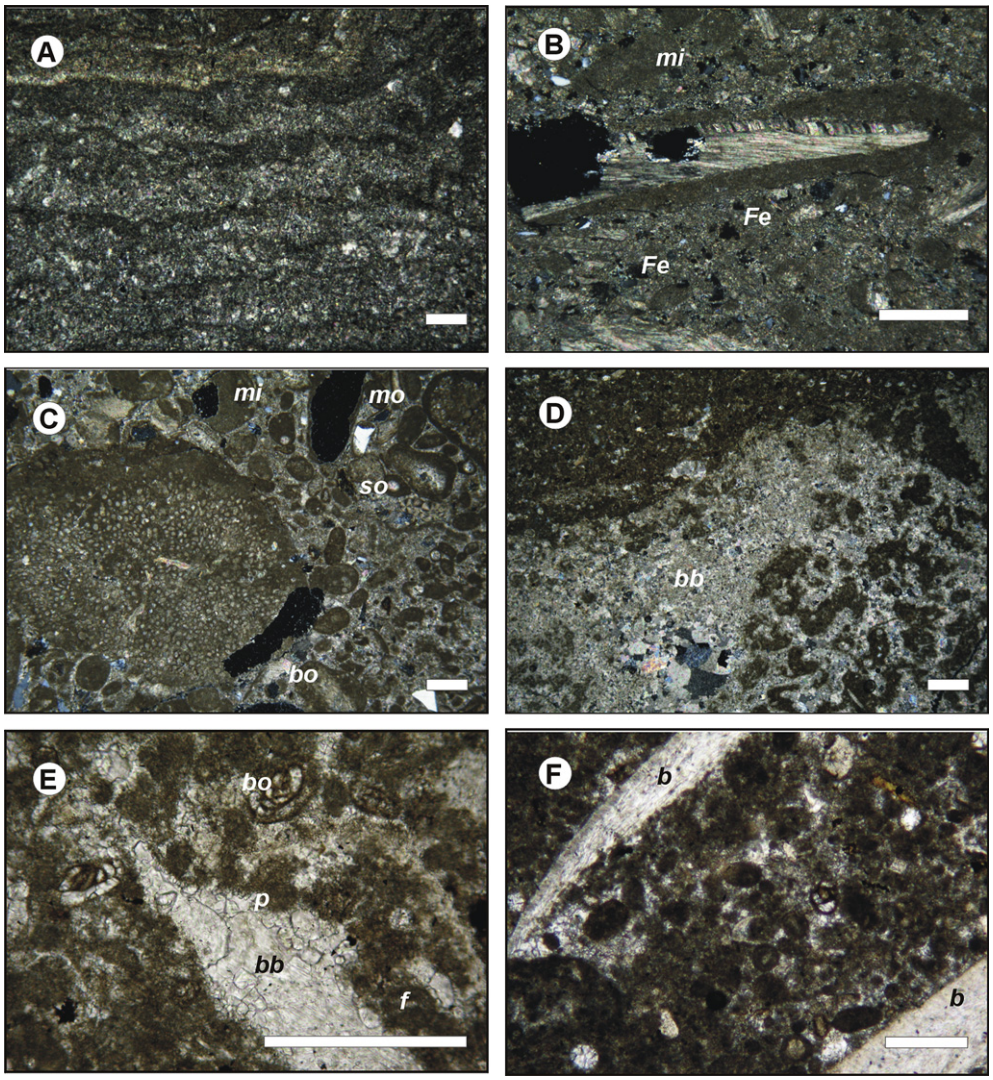

Fig. 7. Photomicrographs of inner ramp microfacies. Scale bars. 200 μm. A: **Stromatolite boundstone** (**B**), subhorizontal microbial lamination, with crenulate contours, micrite laminae with iron oxides in the upper sector. Sample CAP19. B: **Biointraclastic wackestone** (**W3**), brachiopod fragment with endolithic algae cover, micrite intraclasts (mi), peloids, scarce siliciclasts and iron oxide nodules (Fe) scattered in the peloidal micrite matrix. Sample CAVA13. C: **Intraoobioclastic packstone/grainstone** (**P/G2**), algal remain, micrite intraclasts (mi), micrite ooids (mo), siliciclastic nucleus ooids (so), bioclastic nucleus ooids (bo), siliciclasts, rim cement and sparite cement in isopachous fine crystals, with grumous micrite matrix. Sample CAPO13. D: **Bioturbated peloidal wackestone** (**W4**), peloidal micrite matrix affected by a bioturbation burrow (bb) filled with microsparite and sparite cement. Sample CAC8. E: Bioturbated peloidal bioclastic packstone (**P6**), foraminifer section, ooid with foraminifer nucleus (bo), micrite peloids (p), faecal pellets (f) in a peloidal micrite matrix affected by bioturbation burrows (bb). Sample CAC6. F: **Bioturbated peloidal packstone** (**P7**), bivalve shell remains, foraminifer section, micrite peloids, micrite ooids, in a bioturbated peloidal micrite matrix. Sample CAC 10.

upper levels are associated to thin micrite/silty beds, containing abundant fenestras and gypsum crystal casts. Microfacial analysis shows that particles are poorly sorted, main components are intraclasts (25%) composed by micrite or by aggregates of ooids and bioclasts. Ooids (15–25%) are micritic, massive or tangential, and bioclasts (15–20%) correspond to broken bivalves, gastropods, echinoderms, brachiopods, bryozoans, cephalopods, algae remains (dasycladacean and halimedacean) covered by cyanobacteria filaments and scarce faecal pellets. Matrix is made up of grumous micrite with a fine sparite crystalline mosaic cement. Minor gypsum crystals and iron nodules were identified. In La Vaina creek succession, higher matrix contents were observed.

Interpretation: *Fauna and algae association, poorly sorted particles often covered with cyanobacteria filaments and the presence of borings by Glossifungites Ichnofacies suggests low energy sedimentation behind shoals with shallow and clear water conditions. These characteristics define intertidal plains, with unconsolidated substrates, disturbed by tidal action that removed surface sediments. Tidal channels (**P8** and **G3**) transported sediments from shore and basinal areas.*

4.1.3.2. Protected environment facies/microfacies (Calabozo creek section) (Fig. 3).

W4 – Bioturbated peloidal wackestone (Fig. 7D). Beds of 0.20 m–1 m thick present an intense bioturbation consisting of horizontal burrows filled with removed material, organic matter and scattered iron oxide. Unbroken rhynchonellids were observed in the outcroppings and scattered oncoids were identified in the top of the facies. In the upper levels these beds alternate with wackestone and sandy mudstone. This microfacies contains micrite peloids (15%), micrite intraclasts (10%), faecal pellets (5%), micrite ooids and ooids with a siliciclastic nuclei (3%). Bioclasts (5%) include remains of brachiopods, bivalves, echinoderms, foraminifers and dasycladacean algae. Siliciclasts are fine-grained and scarce (5%) and glauconite (1%) was identified in scattered clasts. Matrix is made up of peloidal micrite and bioturbation burrows are filled with fine sparite and microesparite.

Interpretation: *Abundant fine-grained sediment, low fauna diversity, intense bioturbation and the presence of oncoids, suggest a slow accumulation under quite shallow water conditions in a protected environment (lagoon) with ephemeral ponds (mudstone) and inputs from marginal areas.*

P6 – Bioturbated peloidal bioclastic packstone. A 0.60 m thick bed composed of unbroken and broken bivalve shells, outcrops in Calabozo creek succession. Structure is obliterated by intense bioturbation forming a network of orthogonal burrows filled with removed and agglutinate material. This microfacies contains bioclasts (20%) corresponding to rhynchonellids, foraminifer and echinoderm remains (Fig. 7E) and minor micrite peloids (5–10%), micrite intraclasts (5%), ooids (5%), scarce black pebbles (3%) and faecal pellets (3%). Matrix is made up of peloidal micrite with abundant organic matter.

Interpretation: *Biota and abundance of burrows due to annelid worm action indicate intense biological activity in a substrate enriched in nutrients, within a subtidal shallow protected environment. High contents of organic matter and intense bioturbation indicate low sedimentation rate (Flügel, 2004). The presence of ooids and black pebbles suggests sporadic sediment input from shore areas.*

P7 – Bioturbated peloidal packstone (Fig. 7F). Beds approximately 0.80 m thick are strongly disturbed by bioturbation with a characteristic design of irregular subhorizontal burrows and pockets filled with removed material. Rhynchonellid remains, *Entolium* valves and oncoids were identified in the outcrops, which presence decreased remarkably in the upper levels. Scarce scattered undefined plant remains were identified. Particles are mainly composed of micrite peloids and faecal pellets (30–40%); bioclasts (10–20%) corresponding to broken rhynchonellids, bivalves, gastropods, foraminifers, echinoderms and filamentous algae. Scarce oncoids, ooids and scattered glauconite grains were observed. Matrix is made up of grumous bioturbated peloidal micrite with fine-grained sparite cement.

Interpretation: *Particle association, oncoids, glauconite and intense worm bioturbation, suggest a protected subtidal environment with inputs from coastal areas, possibly bays or estuaries. Softground bottoms with abundant organic matter and low sedimentation rate were suitable conditions for detritus feeding activity. These conditions are distinctive of a tidal flat associated to lagoon (Pemberton et al., 1992; Flügel, 2004).*

4.1.3.3. North ramp bar complex facies/microfacies (Serrucho creek and El Plomo creek sections).

G1 – Intrabiooidal grainstone (Fig. 8A). This facies was recognized at the north of the ramp frequently associated to floatstone lentiform bodies (**F4**). Layers 0.30 m–1 m thick are amalgamated and present erosive contact. Bioturbation was recognized at some levels as borings similar to *Ophiomorpha*. In El Plomo creek locality, the base of the beds contains thin intraclastic levels (0.03 m) while at the upper layers high angle cross-stratification and ripples are a very common characteristic. The main components of the microfacies are micrite intraclasts (30–40%), frequently compound; bioclasts (10–20%) represented by fragments of cephalopods, brachiopods, echinoderms, coral, gastropods, bryozoans and foraminifers, dasycladacean algae and *Halimeda*; tangential ooids and micrite oncoids (15–25%). Particles frequently show micrite envelopes (cortoids) and are cemented by blocky sparite with scarce and scattered iron oxide nodules.

Interpretation: *Biota and particle association, residual intraclastic deposits, cross bedding stratification and ripples suggest the deposition of shoal under low energy conditions, distinctive of intertidal areas in shallow waters, affected by continuous wave and current action. Shoals are dissected by tidal channels (**F3**) providing material input from peritidal areas. Stratification was disturbed by infaunal activity.*

F4 – Intrabioclastic floatstone with skeletal wackestone/packstone matrix. This facies is represented by approximately 3.50 m long and 0.20 m–1 m thick lenticular bodies overlying grainstone beds (**G1**) with erosive contact. They present normally graded stratification at the base and swaley cross-stratification with ripples at the top. Particles are reworked and poorly sorted. Intraclasts (30%) and bioclasts (15%) composed of *Weyla* sp., shells and coral are predominantly present. Minor micrite intraclasts, approximately 2 cm in diameter, and siliciclasts were observed. Floatstone matrix is an intrabioclastic wackestone/packstone (Fig. 8B), made up of micrite intraclasts (10%), some from other microfacies, fragmented ooids (5%), oncoids (5%) and peloids (5%). Bioclasts (10%) in El Plomo creek area and 20% in Serrucho creek) are represented by bivalve fragments, frequently covered by endolithic algae, gastropod, bryozoan and algae (*Halimeda*) remains. Matrix is made up of peloidal micrite, with fine sparite cement.

Interpretation: *Bed morphology, structure and reworked particles and bioclasts suggest tidal channels and longshore current facies, associated to shoals (**G1**). Sediments are derived from shoal erosion and peritidal and continental inputs.*

4.1.3.4. South ramp bar complex facies/microfacies (La Vaina creek and Potimalal river sections).

G/P – Oobioclastic grainstones and packstones (Fig. 8C). The inner ramp subenvironment at Potimalal river locality is characterized by this facies, made up of beds 0.30 m–1.90 m thick with normally graded stratification, frequently amalgamated and separated by erosion surfaces. Base levels containing oriented intraclasts and bioclasts are often identified. Layers present bioturbation with

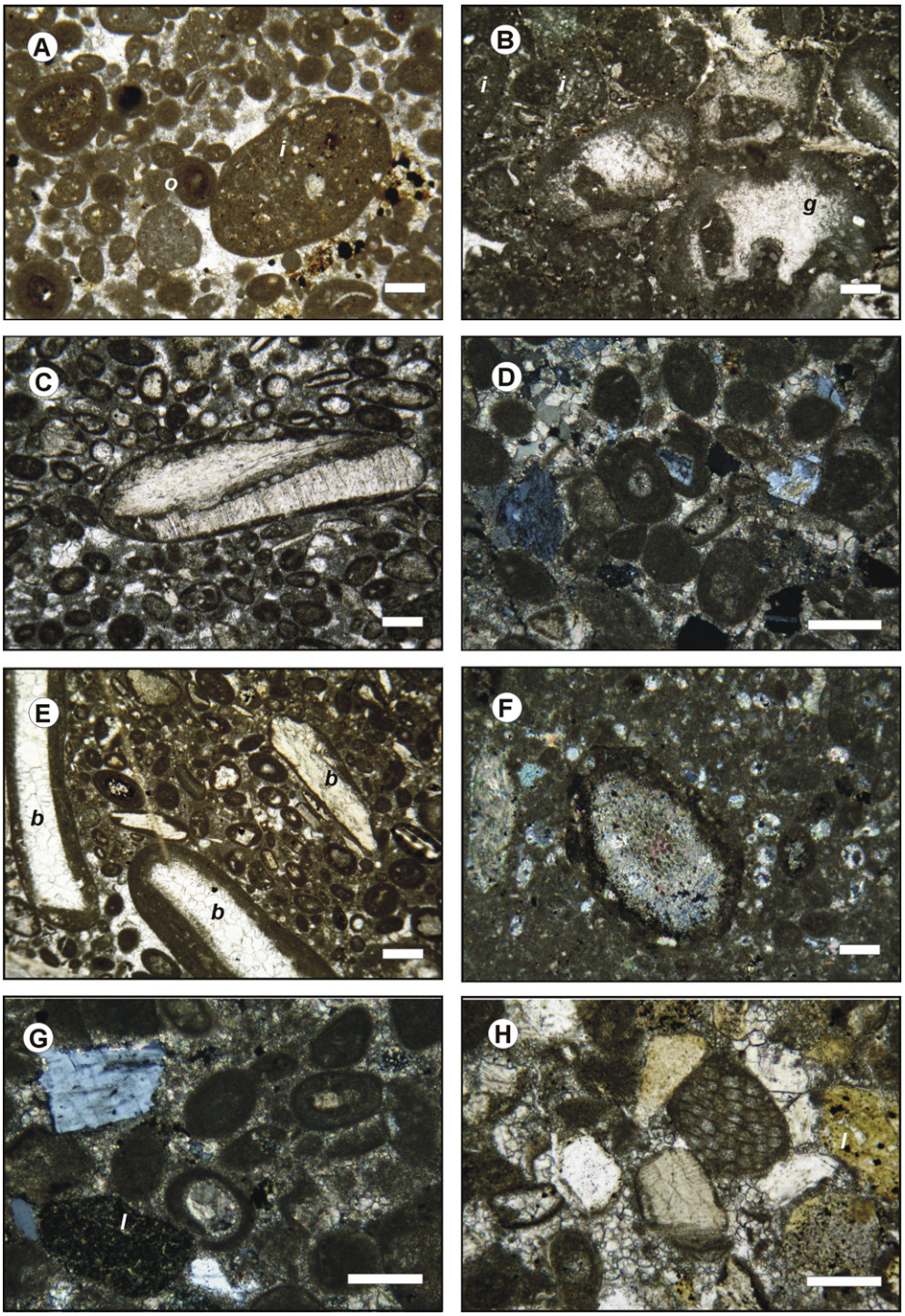

Fig. 8. Photomicrographs of inner ramp microfacies. Scale bars: 200 μm. A: Intrabiooidal grainstone (**G**1), micrite intraclasts composed of other microfacies (i), micrite intraclasts, concentric ooids (o), iron oxide idiomorphic crystals and sparite blocky cement. Sample ASC8. B: Thin section of floatstone (**F4**) matrix, **skeletal wackestone/packstone**, gastropod section (g), micrite intraclasts composed of other microfacies (i), in a peloidal micrite matrix. Sample CAP24. C: **Oobioclastic grainstones and packstones** (**G**/**P**), reworked brachiopod remains covered with endolithic algae cover (b), superficial concentric ooids and micrite ooids, microsparite and sparite blocky cement/blocky cement sparite. Sample CAPO24. D: **Intraoobioclastic grainstone** (**G2**), concentric micrite ooids, micrite ooids, peloids, intraclasts, siliciclasts, rim cement and sparite blocky cement. Sample CAVA9B. E: **Biooidal packstone** (**P8**), bioclasts with thick endolithic algae cover, concentric micrite ooids, micrite intraclasts, peloidal micrite matrix and sparite cement. Sample CAVA12. F: Thin section of rudstone (**R2**) matrix, **bioclastic wackestone/packstone**, reworked bioclasts, echinoderm remains with endolithic algae cover and scattered iron oxide nodules, micrite ooids, superficial ooids with sparite nucleus, micrite intraclasts in a peloidal micrite matrix. Sample CAVA6. G: **Oosiliciclastic grainstone** (**G3**), micrite or sparite nucleus concentric ooids, chloritidized lithoclast (l), micrite intraclasts, angular siliciclasts, iron oxide idiomorphic crystals and sparite blocky cement. Sample CAPO15. H: **Oosiliciclastic grainstone** (**G3**), oogonium, chloritidized lithoclasts (l), micrite intraclasts and sparite blocky cement. Sample CAPO15.

borings to *Ophiomorpha* (*Skolitos* Ichnofacies), *Thalassinoide* (*Glossifungites* Ichnofacies), and horizontal burrows (*Cruziana* Ichnofacies) mainly occur in levels associated to marly shales. This facies is associated to tabular beds from **P/G2** and lenticular bodies corresponding to **G3** and **P8** facies. Gypsum intrasedimentary growth and mudcracks were observed on top of the sequence. The microfacies is characterized by high contents of radial tangential micrite ooids (20–30%) with sparite or bioclastic nucleus, usually presenting oxidized rims, and bioclasts (15–25%) consisting of fragmented bivalves, gastropod (nerineids) and brachiopod remains. Lower quantities of echinoderm, bryozoan, dasycladacean and codiacean algae (*Halimeda*) remains were observed. Siliciclasts are fine-grained (5–15%), intraclasts are micrite or composed of ooid aggregates, some particles are cortoid. Cement is granular sparite (blocky), and matrix is made up of peloidal micrite/microespatite.

Interpretation: *Particles and Ichnofacies association and the presence of oxidized surfaces and gypsum, suggest bars formed in intertidal to peritidal conditions, dissected by channels (**P8**) and associated to tidal flats (**P/G2**). Shoals were affected by strong wave episodes causing erosion and particle detachment. Detrital material input (**G3**) was provided by currents from continental areas. Gypsum crystal growth in the upper levels of the facies implies increased salinity as a consequence of higher shallowing and evaporation conditions in the ramp.*

G2 – Intraoobioclastic grainstone (Fig. 8D). Layers from 0.15 cm to 0.60 cm thick, outcrop in La Vaina creek section. They are frequently amalgamated with erosive surfaces and normally graded stratification. *Ophiomorpha* (*Skolitos* Ichnofacies) bioturbation was observed in the outcrop. Particles are well sorted consisting of well rounded micrite intraclasts (15–25%) and black pebbles; micrite ooids (10–20%) and lower amounts of siliciclasts (5–15%) and micrite peloids (5–10%). Bioclasts correspond to fragmented bivalves, brachipods, echinoderms, bryozoans, coral, fish scale remains and dasycladacean algae. Particles are cemented by blocky sparite.

Interpretation: *Normal grading and good sorting of particles imply depositional conditions in a high energy environment, influenced by wave surf (Cabaleri et al., 2001). Benthonic association, ichnofacies and bioclasts fragmentation indicate normal marine conditions with a sandy substrate in shallow and rough waters (Pemberton et al., 1992).*

P8 – Biooidal packstone. Lentiform layers (1.50 m long and 0.25 m thick) with erosive base and disturbed by *Glossifungites* borings, outcrop in La Vaina creek and Potimalal river sections, the former associated to **P/G2** facies, and the latter associated to **G/P**. The microfacies is characterized by abundant highly broken bioclasts (15–25%), frequently presenting endolithic algae borings (Fig. 8E). Bivalve remains (*Pholadomya* sp.), gastropods (nerineids), echinoderms, and dasycladacean algae remains are predominantly present, along with minor foraminifers. Ooid contents are higher (30%) in La Vaina creek locality and decreases considerably in Potimalal river section (10–15%). The other particles correspond to micrite intraclasts (5–15%) and scarce siliciclasts (1%). Matrix is made up of grumous peloidal micrite/microesparite, and minor radial microcrystalline silica.

Interpretation: *Bed architecture and the presence of Glossifungites indicate a firm ground not yet cemented substrate, characteristic of tidal channels with shore erosion (Pemberton et al., 1992). Particle associations and reworked bioclasts bored by endolithic algae, imply that they are originated in tide influenced areas. These channels cut the tidal flat facies (**P/G2**) in La Vaina creek and the bars (**G/P**) associated to tidal flats (**P/G2**) in Potimalal river.*

G3 – Oosiliciclastic grainstone. This facies is represented by lenticular layers 1.50 m long and 0.20 m–0.40 m thick, with erosive base, swaley crossed stratification and horizontal poorly defined lamination on top, with vertical borings (*Skolitos*). It outcrops in La Vaina creek and Potimalal river localities. In the former, this facies presents erosive contact with rudstone facies **R2** and is covered by **G2** facies. It dissects **P/G2** facies in Potimalal river and underlies beneath G/P facies beds. Microscopic analysis revealed that particles, frequently cortoids, are well sorted and constituted by radial and tangential micrite ooids (25%), angular siliciclasts (20%) and rounded glauconite and chloritidized lithoclasts. Intraclasts are composed of micrite or agglutinated ooids, ranging from 30% in the lower levels to 10% in the upper levels. Bioclasts (10%) are highly broken and include fragments of bivalves, echinoderms, bryozoans, foraminifers, dasycladacean algae, undefined phosphatic remains and scarce oogonium (Fig. 8G and H). Particles are cemented by sparite mosaic and present isopachous crystal growth.

Interpretation: *Bed architecture and particle association indicate channel facies migrating over a tidal flat (**P/G2** facies) in Potimalal river, and over storm deposits in La Vaina creek (**R2**) under intertidal conditions, with remarkable continental and shoal input (**G/P** facies and **G2**).*

4.1.3.5. Storm influenced deposits facies/microfacies (La Vaina creek) (Fig. 3).

R2 – Intraclastic rudstone with bioclastic wackestone/packstone matrix. This facies was identified in La Vaina creek section in contact with **G2** facies at the base, and **G3** on the top. It is made up of 0.20 cm–0.40 cm thick amalgamated layers with erosive bases, normal grading and hummocky cross-stratification. It is characterized by grain supported fabric composed of 2 cm–4 cm in diameter reworked intraclasts (25%), plasticlasts (10%) and bivalve shells (20%) in a bioclastic wackestone/packstone matrix (Fig. 8F). Microscopic analysis allowed the identification of bioclasts (5–10%) corresponding to bivalve remains, gastropods, echinoderms and foraminifers, radial and tangential fragmented ooids (3–10%), micrite peloids, some of algae origin (3–5%), well rounded intraclasts (3%) and scarce siliciclasts. Some particles presented endolithic algae cover, and others presented iron oxide envelopes. Matrix is made up of grumous peloidal micrite, affected by bioturbation with blocky sparite cement filling pore spaces.

Interpretation: *The association of particles from grainstone beds (**G2**) (reworked bioclasts and intraclasts, ooids) and particles from protected environments, possibly tidal flats, (bioclasts and intraclasts with endolithic algae cover, algae peloids, superficial tangential ooids), indicate back shoal deposits affected by bad weather waves.*

4.2. Depositional evolution and facies/microfacies relationships

During the Early Callovian, the back-arc basin in southern Mendoza was flooded by the sea, due to the back-arc subsidence. This marine ingression covered siliciclastic fluvial and marginal marine facies of the Lajas Formation from west Malargüe to southwest Bardas Blancas and defined the change from siliciclastic to carbonatic sedimentation in the region. Analysis of facies and microfacies associations and its lateral and vertical relationships, suggest that marine carbonatic sediments were deposited on an irregular topography inherited from the basement, and highstand conditions were suitable for the development of a homoclinal ramp represented by the Calabozo Formation sequence. Fig. 9 illustrates the reconstruction of the palaeoenvironmental scheme proposed for this ramp. Sedimentation was influenced by sea level fluctuations recorded in shallowing-upward cycles (Cabaleri et al., 2003; Armella et al., 2005a). The base level could have been represented by wave base, like in shallow marine environments (Calvet and Tucker, 1988; Osleger, 1991; Catuneanu, 2006; Catuneanu et al., 2009).

The deepest facies, corresponding to the **proximal outer ramp** subenvironment, widespread in the south of the ramp in Potimalal river locality (Fig. 9A). The lower levels of the sequence correspond to the transition between siliciclastic litoral facies (Lajas Formation) and carbonatic–marine facies (Calabozo Formation). Substrate was

affected by bottom currents that removed organic remains forming bioclastic layers (**P1**) interbedded with thin black shales rich in organic matter. The outer ramp is characterized by an undisturbed substrate composed of black shales and thin mudstone levels (**M**) originated in subtidal environments.

In the north of the Early Callovian basin, a high energy event represents the expansion of the marine domain. This episode is recorded in the grain supported rudstone deposits (**R1**) identified in various localities from south Salado river to north Malargüe river within the **mid ramp** subenvironment. Basal floatstone layers eroded the siliciclastic substrate and reflect the most significant flooding that affected marginal facies of Lajas Formation (Cabaleri et al., 2003). In La Vaina creek area, southwest from Bardas Blancas, the marine sedimentation began under shallow subtidal conditions favourable for the development of benthos. The substrate was disturbed by a high energy episode, possibly storm influenced, that removed and redeposited coarse bioclasts (**F2**) on a residual intraclastic level (lag).

In the north area, to the west of Malargüe, (Fig. 9B) the mid ramp subenvironment is characterized by micrite muds containing abundant nutrients which were deposited under clear and well oxygenated water conditions within the subtidal to intertidal zone. These environmental conditions were suitable for algae growth as well as for the development of biota, mostly bivalves and gastropods. The mainly detrital input (**P2**) was recorded in the Serrucho creek region, probably with source in Lajas Formation marginal facies. These carbonatic sands accumulated in areas strongly disturbed by storms that moved, broke and redeposited particles and organic remains in thin bioclastic levels (**F1**). The muddy substrate (**W/P1**) in the Calabozo creek area was disturbed by low intensity storm waves (**W/P2**) and drained through narrow ephemeral channels (**P5**).

The major mid ramp development was recorded in El Plomo creek region. In this locality, the sequence is characterized by substrates containing abundant nutrients, composed of packstones and grainstones (**P3** and **P/G1**) formed under high energy conditions and by wackestones (**W1**) originated in subtidal zones. These substrates were strongly disturbed by currents and storm waves, and were dissected by channels (**F3**) that carried sediments from ooidal bars and shore areas. The substrate in this region was more intensely affected by bad weather waves, forming the thickest bioclastic storm deposits (**W/P2**) recorded in the ramp. In El Plomo creek section the most sensitivity record of sea level fluctuations was preserved, probably due to a gentler slope, more tidal amplitude and more shallow conditions. Cabaleri et al. (2003) described three shallowing cycles in this locality.

In the south, at Potimalal river section, (Fig. 9A) mid ramp sedimentation occurred under low energy conditions in a subtidal environment with shallow waters, but probably deeper than in the north, with normal oxygen and nutrient contents convenient for the development of oyster and pholadomya benthos. During storm episodes, waves disturbed the soft substrate; organic remains and particles were broken, retransported and accumulated, originating amalgamated bioclastic beds (**W/P2** and **F1**). The smallest mid ramp record was identified in La Vaina creek section. Sedimentation on the packstone substrate (**P4**) was strongly influenced by waves. Based on the low thickness of deposits in this section, we infer they have accumulated over a topographic elevation.

Marginal facies expanded over the entire Early Callovian ramp but became more abundant towards the south (Figs. 3 and 9A and B). Shallowing of the ramp was suitable for the development of an **inner ramp** subenvironment with predominant intertidal and peritidal conditions.

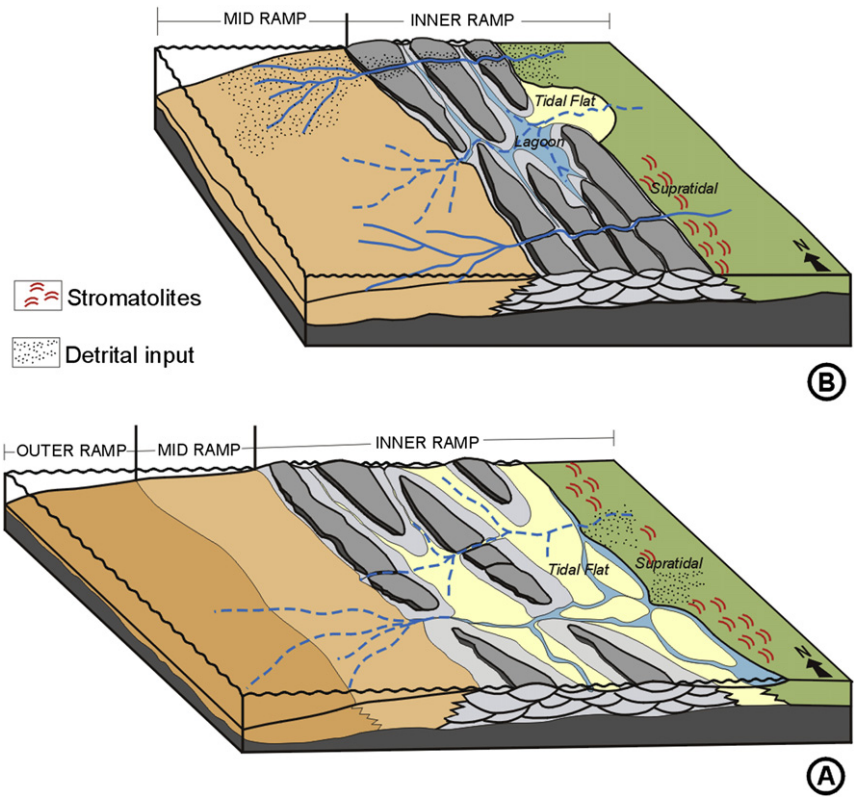

Fig. 9. Palaeoenvironmental scheme of the Early Callovian carbonate ramp from southern Mendoza (Calabozo Formation). A: South ramp area, to the southwestern Bardas Blancas locality. B: North ramp area; to the western of Malargüe locality. Without scale.

In the northern ramp (Serrucho creek and El Plomo creek) sedimentation took place in a tide- and wave-controlled environment, and elongated grainstone bars (**G1**) developed parallel to the shoreline and received detrital input from the continent due to litoral currents. Intertidal channels (**F4**) stored sediments from bar erosion, and allowed the distribution of material from peri, subtidal and continental areas (In Serrucho creek section, plant detritus were found).

In the Calabozo creek area, the inner ramp was characterized by a slow and continued fine-grained sedimentation in a protected subtidal shallow environment containing abundant organic matter. These conditions suggest an embayment of the ramp including the development of lagoon facies (**P6** and **W4**) and tidal flats (**P7**), with shore area inputs. Organic activity was very intense; substrate was strongly disturbed by annelid worms and boring benthos. This environment was highly suitable for the development of brachiopods (rhynchonellids), bivalves (as *Entolium* and rudists), foraminifers, gastropods, echinoderms, ostracods and dasycladacean and filamentous algae.

Inner ramp subenvironment was widespread towards the south, in southwestern Bardas Blancas. Sequences developed in this area were thicker than in the north of the depocenter. In La Vaina creek section, sedimentation was strongly influenced by waves; shoals and grainstone bars formed and were affected by periodic high energy currents and storm waves. Tidal and currents controlled the movement of sediments over the shoals. Material originated by erosion of these bodies and litoral areas, was removed and accumulated in back shoals, forming rudstone levels (**R2**) dissected by channels (**G3**) that redistributed the sediment. Tidal flat deposits (**P/G2** and **W3**) formed between shoals and coastline, and were suitable for the development of bivalves, echinoderms, gastropods and for the growth of filamentous algae and cyanobacteria.

To southwestern La Vaina creek, in Potimalal river, particles were deposited under more shallow conditions, in a high energy environment that broke and disturbed organic remains, forming a grainstone/packstone (**G/P**) shoal and barrier complex that migrated to the coast. This complex was associated with tidal flats (**P/G2**) and ephemeral ponds where very fine-grained sediments (marls and shales) accumulated. Sediments from marginal and continental areas were transported and redistributed by the tidal channels (**P8** and **G3**), that migrated on flats and dissected the shoals. These channels connected marginal areas with the deeper facies, and allowed ocean current inputs into tidal flats.

The development of fringing shoals, followed by coastline migration resulted in a subaerial exposure of the shoals and a progressive isolation of the basin. Aridity as well as high temperature and shallowness, were suitable conditions for evaporation. In El Plomo creek, La Vaina creek and Potimalal river areas, shoal and tidal flat facies change laterally to shales with anhidrite. Increased evaporation and salinity in the environment created unsuitable conditions for the development of benthonic fauna and algae (dasycladacean and halimedacean). Only benthonic microbial communities which adapted to extreme conditions survived and built up stromatolites (**B**) interbedded with anhidrite levels. These evaporatic levels indicate more restricted environmental conditions and the beginning of carbonatic/evaporitic sedimentation, distinctive of the Tábanos Formation (Callovian) sequence.

5. Isotope and geochemical data

5.1. Results

One of the objectives of this paper was to link the detailed sedimentological study with the geochemical data and specifically, to interpret the isotope variations in shallow marine carbonates. Results are summarized in Table 4.

Carbon and oxygen isotopic composition of bulk rock carbonates is used to interpret the variations in oceanic isotopic signals. The variability of carbon and oxygen isotope composition of seawater is greatest in the shallow coastal zones because of significant evaporation, freshwater discharges and carbon transfer. An inadequate understanding of this variability, as well as different diagenetic environments, limit the interpretation of the stable isotope record of shoal water carbonates. On the other hand, the application of strontium-isotope ($^{87}Sr/^{86}Sr$) stratigraphy to carbonate sequences has been extensive as correlation and dating tool. When applied to platform carbonate rocks, Sr isotopes can provide an indication of the exchange with global marine waters.

Key elements (Sr, Rb, Mn and Fe) have been analyzed in order to detect the influence of diagenesis. Diagenesis normally leads to depletion in Sr and enrichment in Mn and Fe contents (Brand and Veizer, 1980). Sr^{2+} and Mn^{2+} are used as diagenetic tracers due to their widely divergent partition coefficients, association with the carbonate lattice, and large compositional differences in marine and meteoric water (Colombié et al., 2011). Samples with Mn/Sr > 2 usually have altered isotopic compositions, while those with lower values yielded quite consistent results (Jacobsen and Kaufman, 1999). Various Fe and Mn content limits have been applied to exclude altered samples (Anderson et al., 1994; Denison et al., 1994; Ditchfield, 1997; Rosales et al., 2004). Nevertheless, universal threshold values for these chemical criteria are difficult to adopt since the sedimentary, early diagenetic and late diagenetic chemical environments are different for each sediment (Žák et al., 2011).

5.2. Discussion

5.2.1. Carbon and oxygen isotopes

5.2.1.1. Data span and variability. The range of $\delta^{13}C$ and $\delta^{18}O$ values shows considerable differences between individual sections. In the Serrucho creek section, carbon isotope values ($\delta^{13}C$) range from $-0.2‰$ to $+0.3‰$ and $\delta^{18}O$ values from $-10.1‰$ to $-5.2‰$. A positive $\delta^{13}C$ shift towards a maximum of $+3.6‰/+3.9‰$ occurred upward in the section accompanied with an increase in $\delta^{18}O$ ($-4.0‰$). In the El Plomo creek section, the carbon isotopic composition through the carbonate succession varies from $0.7‰$ to $2.0‰$ and the $\delta^{18}O$ values from $-11.7‰$ to $-9.9‰$. In Arroyo La Vaina section carbon isotopic values do not show a high span, varying from $0.6‰$ to $1.1‰$ and $\delta^{18}O$ ranges from $-9.7‰$ to $-6.5‰$. A positive shift to heavier $\delta^{13}C$ ($+3.6‰/+3.9‰$) with an increase in $\delta^{18}O$ ($-4.0‰/-5.3‰$) were recorded close to the top of the sequence. Finally, the $\delta^{13}C$ values in the Potimalal river sections range from $-1.0‰$ to $2.2‰$, while the $\delta^{18}O$ varies from $-11.1‰$ to $-5.6‰$.

5.2.1.2. General patterns. As can be seen in Fig. 10 there is no systematic variation in $\delta^{13}C$ and $\delta^{18}O$ values according to the depositional setting and facies associations so, it is not possible to delineate facies based on the $\delta^{13}C$ and $\delta^{18}O$ values. Evidently, these shallow marine carbonates developed their own isotopic signature influenced by local palaeoenvironmental parameters and were variably prone to significant alterations of their original marine isotopic signal during exposure and/or during early to late diagenesis. Correlations are poor for all the studied sections and there are no clear spatial trends in the carbon and oxygen isotopic values of sediments with Fe concentrations and Mn/Sr ratios (Fig. 11A–D). Considering these characteristics, each section is individually treated, taking into account local paleoenvironmental conditions and post-depositional histories.

Table 4
$\delta^{13}C$ and $\delta^{18}O$ values, Rb, Sr, Fe and Mn contents, Mn/Sr ratios and $^{87}Sr/^{86}Sr$ ratios from Serrucho (samples ASC), El Plomo (samples CAP), La Vaina (samples CAVA) and Potimalal (samples CAPO) sections. Data of each section are presented in stratigraphic order.

Section	Sample	Facies	$\delta^{13}C$ (±0.1) (‰)	$\delta^{18}O$ (±0.1) (‰)	Rb (ppm)	Sr (ppm)	Fe (%)	Mn (ppm)	Mn/Sr	$^{87}Sr/^{86}Sr$ (±1σ)
Serrucho creek	ASC10	**G1**	3.6	−4.0	5	284	0.38	284	0.71	
	ASC9	**G1**	3.9	−5.3	<2	379	0.42	379	0.63	
	ASC8	**G1**	0.0	−10.6	<2	267	1.06	267	1.02	
	ASC7	**F1**	0.2	−10.1	28	332	1.28	332	0.93	
	ASC6	**P2**	0.3	−7.5	23	275	1.86	275	1.59	
	ASC3	**P2**	0.1	−9.7	39	297	2.25	297	0.85	
	ASC1	**R1**	−0.2	−5.2	<2	241	0.43	241	1.63	
El Plomo creek	CAP19	**B**	1.1	−10.1	x	377	0.086	85	0.23	
	CAP25	**G1**	0.7	−11.5	x	268	0.121	968	3.61	
	CAP23	**G1**	1.2	−10.8	x	360	0.120	224	0.62	0.706900 ± 24
	CAP24	**F4**	1.1	−11.1	x	408	0.158	170	0.42	
	CAP17	**G1**	1.6	−11.1	x	398	0.084	147	0.37	
	CAP15	**G1**	1.0	−10.0	x	352	0.171	248	0.70	
	CAP14	**P/G1**	0.9	−9.9	x	423	0.209	434	1.03	
	CAP13	**W1**	1.4	−11.1	x	387	0.423	441	1.14	
	CAP12	**W1**	0.8	−10.8	x	298	0.309	588	1.97	
	CAP11	**P3**	1.4	−10.7	x	366	0.245	480	1.31	
	CAP10	**W/P2**	1.4	−10.6	x	374	0.110	124	0.33	
	CAP9	**W/P2**	1.8	−11.2	x	549	0.110	124	0.23	0.706923 ± 23
	CAP8	**F3**	2.0	−10.9	x	379	0.343	108	0.28	
	CAP6	**P3**	2.0	−11.1	x	514	0.266	178	0.35	0.707134 ± 22
	CAP5	**W1**	2.0	−11.3	x	440	0.365	116	0.26	
	CAP4	**W1**	1.9	−11.1	x	540	0.247	163	0.30	
La Vaina creek	CAVA30	**B**	3.0	−5.5	x	235	0.69	604	2.57	
	CAVA13	**W3**	1.1	−6.5	x	160	0.8	271	1.69	
	CAVA11	**P/G2**	0.1	−9.7	x	165	0.11	449	2.72	
	CAVA10	**P/G2**	0.6	−9.4	x	212	0.15	387	1.83	
	CAVA9	**G2**	0.6	−9.4	x	145	0.55	372	2.56	
	CAVA7	**R2**	1.1	−8.9	x	150	0.38	341	2.27	0.706934 ± 14
	CAVA5	**G2**	0.7	−9.0	x	150	0.61	395	2.63	
	CAVA3	**P4**	0.6	−8.7	x	142	0.38	403	2.84	
	CAVA1	**F2**	0.9	−8.6	x	181	0.52	434	2.4	0.706990 ± 24
Potimalal river	CAPO27	**G/P**	1.7	−9.0	<5	173	0.3	240.0	1.4	0.706888 ± 21
	CAPO26	**G/P**	1.7	−8.9	<5	168	0.3	248.0	1.5	
	CAPO19	**P/G2**	0.8	−8.1	<5	156	0.2	256.0	1.6	
	CAPO25	**P8**	1.5	−7.3	23	153	1.2	248.0	1.6	
	CAPO24	**G/P**	1.6	−7.1	9	162	0.4	186.0	1.1	
	CAPO17	**G/P**	1.5	−8.5	<5	186	0.5	240.0	1.3	
	CAPO14L	**G/P**	2.0	−9.5	<5	209	0.2	240.0	1.1	0.706953 ± 20
	CAPO21	**G3**	1.5	−8.3	23	154	0.5	248.0	1.6	
	CAPO20	**G3**	1.7	−7.9	27	206	0.6	217.0	1.1	0.706986 ± 22
	CAPO15	**G3**	x	x	x	x	x	x	x	0,707134 ± 13
	CAPO13	**P/G2**	1.2	−8.7	18	184	0.6	248.0	1.3	0.707057 ± 29
	CAPO12	**F1**	0.7	−10.9	x	x	x	x	x	
	CAPO18	**W1**	x	x	8	148	8.000	232	1.57	0.706999 ± 20
	CAPO11	**W1**	1.3	−8.1	9	173	0.7	263.0	1.5	
	CAPO10	**W2**	1.3	−8.1	7	205	0.6	287.0	1.4	
	CAPO9	**W/P2**	0.8	−7.1	12	169	1.3	294.0	1.7	
	CAPO8	**W2**	0.7	−7.3	34	152	1.0	256.0	1.7	
	CAPO7	**W/P2**	1.0	−6.9	20	198	0.7	294.0	1.5	
	CAPO6M	**M**	0.2	−6.6	29	143	1.2	318.0	2.2	
	CAPO6	**M**	−0.3	−5.8	24	149	0.9	279.0	1.9	
	CAPO5	**M**	0.1	−5.6	28	141	0.7	263.0	1.9	
	CAPO2	**P1**	−1.1	−7.6	10	153	0.4	403.0	2.6	

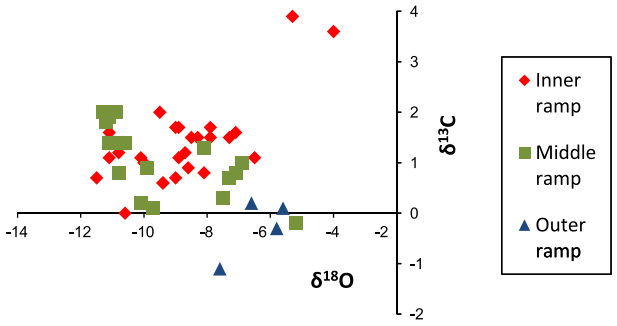

Fig. 10. Scatter diagram $\delta^{13}C$ *vs* $\delta^{18}O$ for samples of Calabozo Formation according to the ramp subenvironments.

Serrucho creek In the Serrucho creek section (Fig. 12), a depleted $\delta^{13}C$ value (−0.2‰) characterizes the lower levels (**R1**). This facies represents the marine ingression, which affected the marginal marine/deltaic plain of Lajas Formation. Isotopic values of carbon increase upward in the section to 0.1–0.3‰ (facies **P2**) in carbonates accumulated in a subtidal environment. The lowest value (0.0‰) was registered in shoal deposits developed in the intertidal area (inner ramp). A positive shift of $\delta^{13}C$ values towards a maximum of 3.6–3.9‰ was registered in the upper levels of the section, in shoal deposits of peritidal areas (facies **G1**). The stromatolite fragments with interstitial gypsum (facies **B**) recognized over these levels, indicate evaporation conditions and increased salinity. $\delta^{18}O$ values are depleted and scattered ($-4.0‰ \leq \delta^{18}O \leq -10.6‰$) with a positive shift (−4.0‰/−5.3‰)

towards the top of the section which correlates with the shift of $\delta^{13}C$ values. Oxygen isotope ratios are quite depleted in comparison with those of coeval unaltered marine carbonates.

The depleted $\delta^{13}C$ value of the lower levels is interpreted as the result of the oxidation of continental organic matter (deltaic plain) to CO_2 to form bicarbonate, which precipitation results in carbonates with negative isotope signal. The $\delta^{13}C$ values of the inner ramp facies are typical of marine limestones. The $\delta^{13}C$ positive shift towards the top of the section is interpreted as an indicator of a change in the environmental conditions. Many authors reported a $\delta^{13}C$ positive shift in western Tethyan seaway deposits of the Early Callovian of the Apennines, Italy, (Morettini et al., 2002; Bartolini et al., 1999) but the simultaneous $\delta^{13}C$–$\delta^{18}O$ increase in Serrucho creek, suggests that it probably represents a local shoal water event (evaporation). Cabaleri et al. (2001) defined, on the basis of facies/microfacies analysis and geochemical data, a progressive isolation of the basin which allowed the establishment of strong evaporative conditions that promote chemical precipitation of gypsum of the Tábanos Formation. In increasingly saline waters, the remaining dissolved CO_3H^- became progressively enriched in ^{13}C and ^{18}O which precipitation results in isotopically enriched carbonates. Taking into account these evidences, this shift cannot be correlated with the deepening pulse suggested for Callovian times by other authors on the base of the carbon isotope excursion recorded in pelagic sediments of Italy (Morettini et al., 2002; Bartolini et al., 1999).

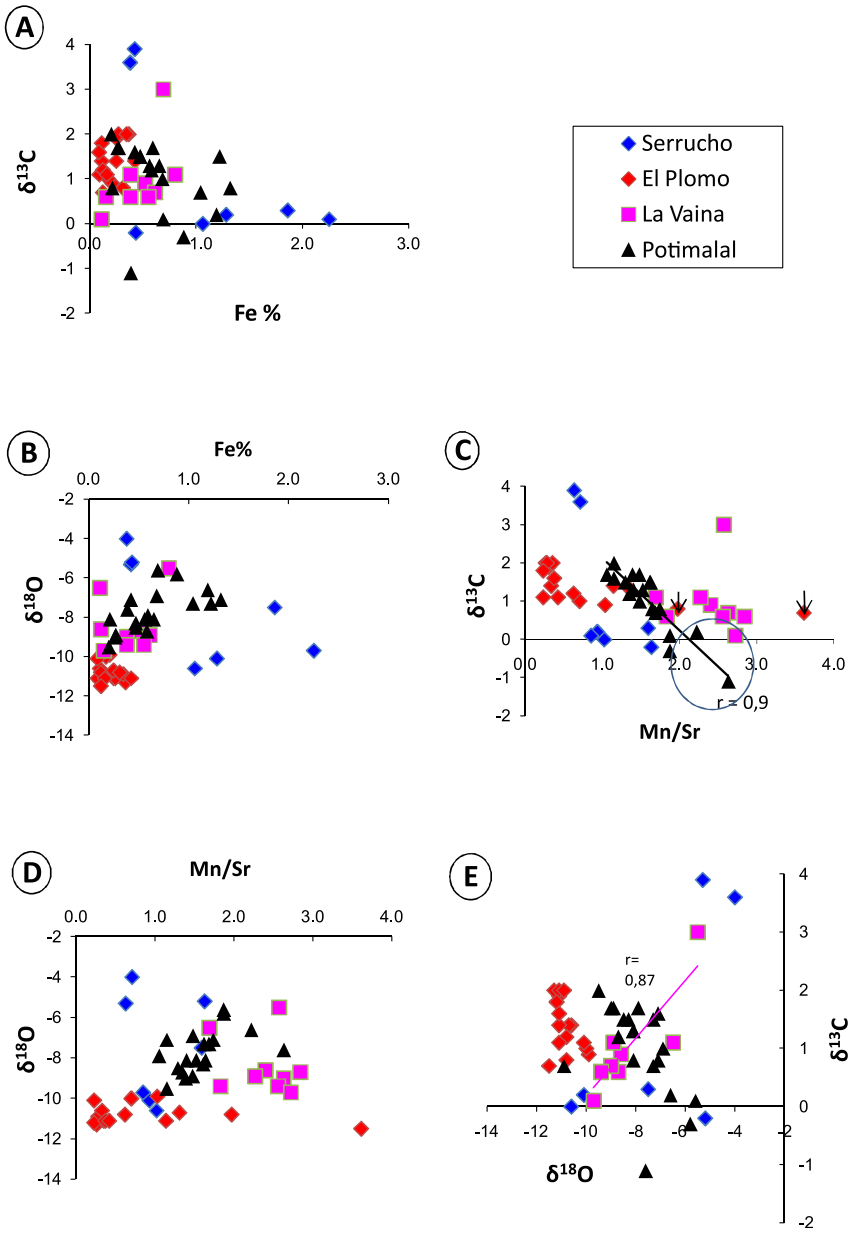

Fig. 11. Scatter diagrams: A: $\delta^{13}C$ *vs* Fe contents (%) for samples of Calabozo Formation from Serrucho, El Plomo, La Vaina and Potimalal sections. B: $\delta^{18}O$ *vs* Fe contents (%) for samples of Calabozo Formation from Serrucho, El Plomo, La Vaina and Potimalal sections. C: $\delta^{13}C$ *vs* Mn/Sr ratios for samples of Calabozo Formation from Serrucho, El Plomo, La Vaina and Potimalal sections. Only two samples from El Plomo section have high Mn/Sr ratios (see arrows). Within the Potimalal section, outer ramp samples show the highest Mn/Sr ratios (closed area). $\delta^{13}C$ values and Mn/Sr ratios have good correlation in the Potimalal river section ($r = 0.9$). D: $\delta^{18}O$ *vs* Mn/Sr ratios for samples of Calabozo Formation from Serrucho, El Plomo, La Vaina and Potimalal sections. E: ^{13}C *vs* $\delta^{18}O$ for samples of Calabozo Formation from Serrucho, El Plomo, La Vaina and Potimalal sections. $\delta^{13}C$ and $\delta^{18}O$ values correlate in La Vaina creek section ($r = 0.87$). Samples from El Plomo creek section have the more negative $\delta^{18}O$ values.

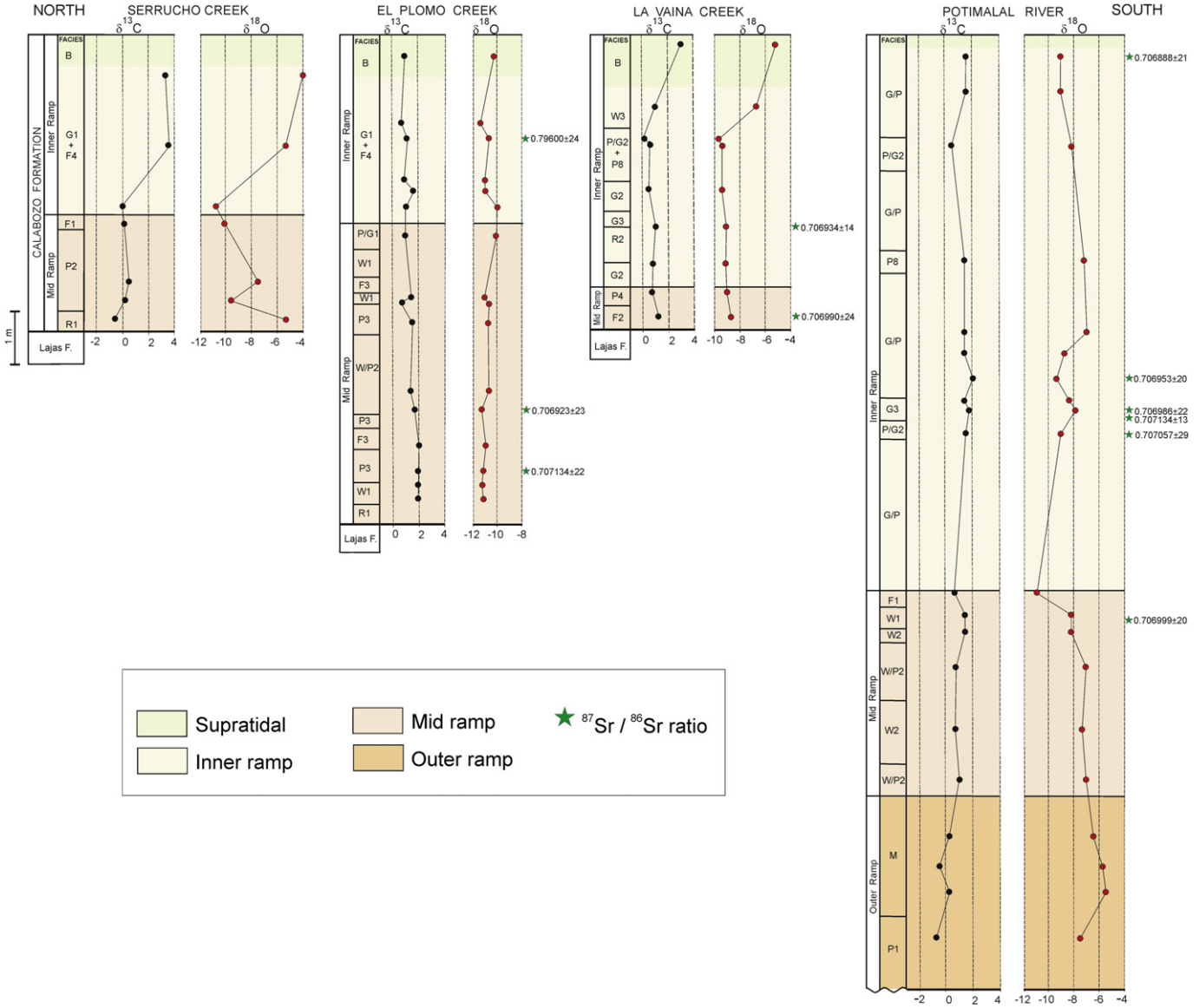

Fig. 12. Vertical variation of facies, $\delta^{13}C$, $\delta^{18}O$ and $^{87}Sr/^{86}Sr$ data in the different studied sections. The horizontal distances between sections are not to scale.

El Plomo creek In El Plomo creek two sections were studied but they were summarized in one columnar section (Fig. 12). The carbon isotopic composition through the succession varies from 0.7‰ to 2.0‰ and $\delta^{18}O$ values from −11.3‰ to −9.9‰. This sequence revealed higher sensitivity to sea level fluctuations than the rest of the ramp, probably due to gentler slope and longer tidal amplitude. Cabaleri et al. (2003) described three shallowing cycles for this locality.

The carbon-13 composition at the lower part of the section (mid ramp facies, **W1**, **P3** and **F3**) is almost constant (1.9–2.0‰). Upward, $\delta^{13}C$ values range from 1.8‰ to 1.4‰, in shallow subtidal deposits disturbed by storm episodes (facies **W/P2**). These episodes of high hydrodynamic energy, probably originated detrital inputs from the continental margin with small amounts of isotopically light carbon derived from the oxidation of organic matter (Valencio et al., 2003). The shallowing cycles, with repeated episodes of organic matter oxidation, subaerial exposition and evaporation, controlled the $\delta^{13}C$ variations in the upper part of the section (inner ramp), with a range of values from 0.7‰ to 1.6‰ (facies **G1** + **F4**). The $\delta^{18}O$ mean value (−10.9‰) for the carbonates of this section is the most negative.

Limestones of El Plomo creek have the highest Sr contents and lower Mn/Sr ratios, indicating that they were less affected by the interaction with diagenetic fluids. $\delta^{13}C$ values (1.1–2.0‰) are close to the estimated range for Callovian unaltered marine carbonates (Valencio et al., 2003). In only two samples (facies **W1**, **G1**), the isotope signature (0.8‰ and 0.7‰) could be weakly influenced by meteoric waters as they have the highest Mn/Sr ratios (Table 4, Fig. 11C). While $\delta^{13}C$ values are typically marine, the oxygen isotopic compositions are very depleted (mean value = −10.9‰). Valencio et al. (2003) suggest an interaction with meteoric waters, like water coming from high altitude. However, an alternative explanation like recrystallization and ^{18}O depletion due to elevated temperatures during burial diagenesis and orogeny (Veizer et al., 1999) cannot be discharged. Considering the lowest Mn/Sr ratios of El Plomo carbonates (Fig. 11C) and no significant changes in the $\delta^{13}C$ values, the second hypothesis seems the more likely interpretation.

La Vaina creek The samples from La Vaina creek section have the strongest evidences of post-depositional changes. The isotopic values do not show a high span ($0.6‰ \leq \delta^{13}C \leq 1.1‰$ and $-9.7‰ \leq \delta^{18}O \leq -6.5‰$) through the whole sequence and, going up to the supratidal facies, a positive shift of $\delta^{13}C$ and $\delta^{18}O$ values were recorded close to the top of the sequence (facies **B**, Fig. 12).

The carbonates of La Vaina creek section present the highest Mn/Sr ratios (Fig. 11C) and a good correlation trend between $\delta^{13}C$ and $\delta^{18}O$ values ($r = 0.87$) (Fig. 11E), indicating that they probably do not reflect the original isotope composition and merely in this section, carbon and oxygen isotope ratios were modified in the same way. The $\delta^{13}C$–$\delta^{18}O$ positive shift at the top of the succession is associated to the strong evaporative conditions due to the progressive isolation of the basin (Cabaleri et al., 2001).

Potimalal river In the Potimalal river two sections were studied. According to the good correspondence between $\delta^{13}C$ variations and facies in the outcrops at both river margins, they were summarized in one columnar section (Fig. 12). Only in Potimalal river section, outer ramp facies (facies **F1**, **M1**) are registered. These facies were expected to record the primary open marine carbon isotope signal as they are less affected by environmental processes (evaporation, continental inputs, carbon transfer) (Wissler et al., 2003). However, they have depleted $\delta^{13}C$ values ($-1.1‰$–$0.2‰$). The $\delta^{13}C$ values recorded in the mid ramp facies span between $0.7‰$ (facies **W2**, **F1**) and $1.3‰$ (facies **W1**, **W2**). The lowest carbon isotopic ratios within the mid ramp were recorded in subtidal/intertidal deposits affected by storm episodes. The $\delta^{13}C$ values of the inner ramp facies are slightly higher (1.5–$1.7‰$). A value of $2‰$ was obtained in bar carbonates developed in intertidal to peritidal conditions (facies **G/P**). The $\delta^{18}O$ values in the Potimalal river section vary from $-11.1‰$ to $-5.6‰$.

The linear correlation ($r = 0.90$) between $\delta^{13}C$ values and Mn/Sr ratios suggests that these carbonates could have altered marine isotopic signals. Moreover, Mn/Sr ratios are higher in the outer ramp facies (Fig. 11C), suggesting strong burial and meteoric diagenetic alteration for these samples. The depletion of the carbon isotope ratios ($\delta^{13}C$: -1.1–$0.2‰$) of these samples could be explained by fluid–rock interactions driven by advection of fluids enriched in organic matter during burial and sediment compaction. This process involves oxidation of previously deposited organic matter to form a source of ^{13}C-depleted carbonate cements (Grotzinger et al., 2011). The $\delta^{18}O$ values are also depleted but show poor correlation with Mn/Sr ratios (Fig. 11D).

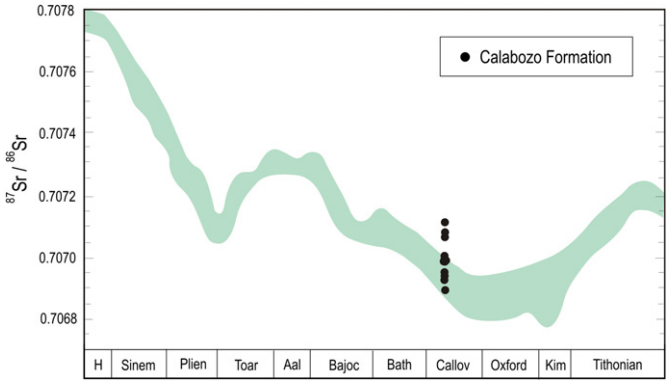

Fig. 13. Strontium-isotope curve for Jurassic seawater (adapted from Jenkyns et al., 2002) and strontium-isotope data of Calabozo Formation limestones.

5.2.1.3. Concluding remarks. Most of the $\delta^{13}C$ values in Calabozo Formation are close to the documented range of Callovian marine limestones (≈ 0.5–$4‰$, Jenkyns et al., 2002). El Plomo creek section has the best preserved $\delta^{13}C$ record while La Vaina creek section has the strongest evidences of post-depositional changes. The $\delta^{18}O$ values are always negative ($-11.7‰$ to $-5.2‰$) and are lower than the literature estimates of Callovian marine carbonates.

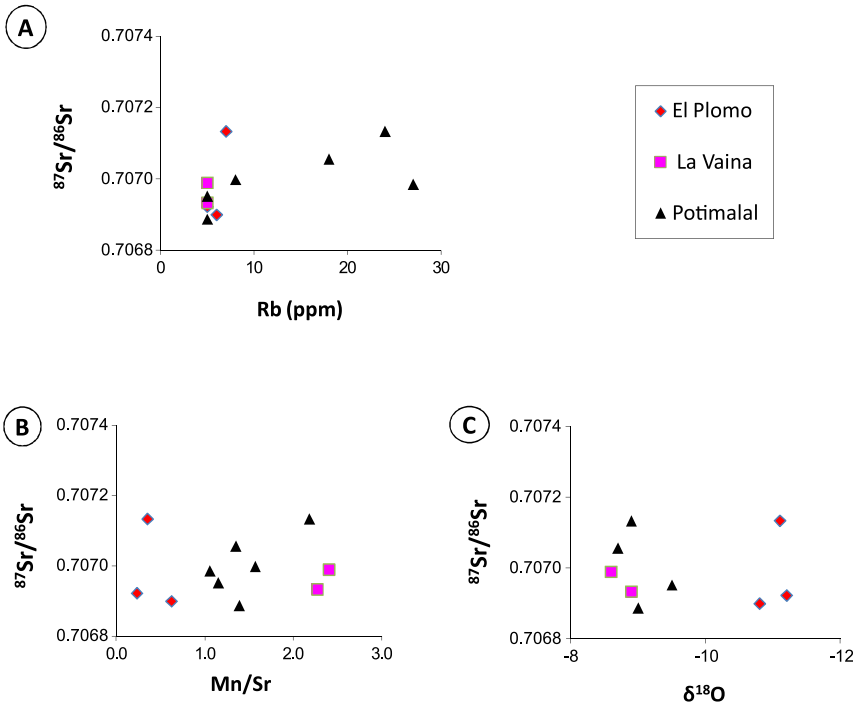

Fig. 14. Scatter diagrams: A: $^{87}Sr/^{86}Sr$ ratios *vs* Rb contents for samples of Calabozo Formation from El Plomo, La Vaina and Potimalal sections. B: $^{87}Sr/^{86}Sr$ *vs* Mn/Sr ratios for samples of Calabozo Formation from El Plomo, La Vaina and Potimalal sections. C: $^{87}Sr/^{86}Sr$ ratios *vs* $\delta^{18}O$ values for samples of Calabozo Formation from El Plomo, La Vaina and Potimalal sections.

Paleoenvironmental conditions have influenced the isotope signal in all the sections. Furthermore, the diversity of facies with different initial porosities, permeabilities and reactivities in relation to diagenetic fluids, are also reflected in the $\delta^{13}C$ and $\delta^{18}O$ oscillations between carbonates of the different studied sections.

5.2.2. Strontium isotopes

Most of the Sr isotopic ratios are in agreement with the Callovian seawater Sr-isotope curve (Fig. 13) although some scattered values towards more radiogenic contents, probably indicate variable modifications of the primary isotopic signal (Cagnoni et al., 2006). The plots of $^{87}Sr/^{86}Sr$ versus the diagenetic tracers (Rb contents, Mn/Sr ratios and $\delta^{18}O$ values, Fig. 14A–C) reveal variable correlations reinforcing the idea of changes in diagenetic alteration from one section to the other. The availability and spatial distribution of certain elements in the diagenetic system have controlled the exchange during fluid–rock interactions. The Jurassic isotope curve has been constructed mainly based on results from carbonate sequences in the Tethyan province. In the Mid and Late Jurassic, the Hispanic Corridor was a narrow open marine connection from western Tethys across Central America into western South America (Hallam, 1983). Palaeontological studies have strongly indicated that this seaway was opened during the Early Jurassic and its continuously open nature, allowed the free interchange of marine biotas between the western Tethys and the eastern Pacific oceans (Westermann and Riccardi, 1985; Aberhan, 2001; Riding et al., 2011). The agreement of the strontium isotopic record of the Calabozo Formation with the global $^{87}Sr/^{86}Sr$ curve, indicates that the Hispanic Corridor connectivity allowed water-mass exchanges. The exchange between the shallow carbonate ramp and open marine waters makes the Calabozo Formation strontium isotopic record representative of the Callovian global ocean.

6. Conclusions

The Early Callovian ingression, which affected the Neuquén basin in southwestern Mendoza, is represented by the shallow marine facies of the Calabozo Formation carbonate sequence. The distribution of studied facies indicates sedimentation conditions on a gentle slope, distinctive of a homocline ramp profile, without breaks or evidence of gravitational deposits. The thickness variation in the Calabozo Formation reflects a topographic control over the marine sedimentation, and a considerable development of the ramp towards the south.

The vertical distribution of facies, the ramp evolution involving development of outer, mid and inner ramp subenvironments, the reduced siliciclastic input, and the predominant inner ramp subenvironment with peritidal facies in the upper levels, indicate that the Calabozo Formation developed during a highstand stage. Starting conditions during the Early Callovian marine ingression were suitable for the development of a mid ramp subenvironment except in the south of the depocenter (Potimalal river) where carbonatic sedimentation began in an outer ramp subenvironment. This subenvironment is defined by low energy proximal outer ramp facies. Base levels originated in a moderate energy subenvironment reflecting the transition between Lajas and Calabozo formations.

Sedimentation within the mid ramp subenvironment took place under subtidal/intertidal conditions. The increased oxygenation allowed the development of benthonic fauna and dasycladacean algae. The most conspicuous development of the mid ramp was identified in El Plomo creek area, where the substrate was strongly affected by storm waves resulting in the thickest tempestite deposits. At this locality, the gentle slope is supposed to have generated an extensive ramp, with large intertidal amplitude and more shallow conditions, sensitive to sea level variations.

The deepest mid ramp subenvironment facies, associated to marly shale sediments containing detrital input, were identified in Serrucho creek and Potimalal river localities, north and south of the ramp respectively.

The inner ramp subenvironment expanded over the entire ramp however, the sections are thicker towards the south (La Vaina creek and Potimalal river localities). In the north, the inner ramp is characterized by a complex of elongated shoals cut by tidal channels. Protected environment facies were identified in the Calabozo creek area indicating a local embayment. In the southern depocenter the inner ramp is represented by a fringing shoal complex which migrated over tidal flats dissected by channels, where ponds containing fine sediment (marls and shales) with shore area inputs, were formed.

Paleoenvironmental evolution of the Calabozo Formation resulted in a progressive isolation of the basin and the almost entire depocenter dessication. Increased evaporation and salinity provided unsuitable conditions for the development of benthonic fauna and algae. Only benthonic microbial communities which adapted to such extreme conditions survived. The beginning of the carbonatic/evaporitic sedimentation of Tábanos Formation (Callovian) is evidenced by the development of stromatolites interbedded with gypsum levels.

Most of the $\delta^{13}C$ values from Calabozo Formation are close to the documented range of Callovian marine limestones ($\approx 0.5-4‰$). El Plomo creek section has the best preserved $\delta^{13}C$ record, while La Vaina creek section has the strongest evidences of post-depositional changes. The $\delta^{18}O$ values are always negative ($-11.7‰$ to $-5.2‰$) and lower than the literature estimates of Callovian marine carbonates.

The diversity of facies with different initial porosities and permeabilities and different reactivities in relation to diagenetic fluids, is reliably reflected in the $\delta^{13}C$ and $\delta^{18}O$ oscillations between the carbonates of the different studied sections. Paleoenvironmental conditions have influenced the carbon and oxygen isotope signal in all the sections. The geochemical and isotope data show that, in a shallow water context, the isotopic composition of the bulk carbonates are a composite signal resulting from a complex combination of local, regional and probably global effects. Therefore, carbon and oxygen isotope records can be used as a tool for stratigraphic correlations only when the origin of the isotopic signals is well understood.

The $^{87}Sr/^{86}Sr$ ratios are in agreement with the Callovian seawater Sr-isotope curve. This agreement indicates that the ocean connectivity allowed water-mass exchanges and the exchange between the shallow ramp and open marine waters makes that isotopic record representative of the Callovian global ocean.

Acknowledgements

This research was supported by CONICET (Grant PEI 6461) and ANPCyT (Grant PICT 07-12128). The authors are grateful to Lic. Adriana Ramos for her valuable help and advice during the course of this study, especially with the geochemical analysis. We acknowledge Mr. G. Giordanengo who made the illustrations and Mr. E. Llambias for preparing the petrographical thin sections. Finally, this paper is dedicated to the memory of our friend Susana Valencio.

References

Aberhan, M., 2001. Bivalve palaeobiogeography and the Hispanic corridor: time of opening and effectiveness of a proto-Atlantic seaway. Palaeogeography, Palaeoclimatology and Palaeoecology 165, 375–394.

Adams, A., Mackenzie, W., Guilford, C., 1995. Atlas of Sedimentary Rocks under the Microscope, fifth ed. Longman Scientific &Technical, Hong Kong, p. 104.

Anderson, T.F., Popp, B.N., Williams, A.C., Ho, L.Z., Hudson, J.D., 1994. The stable isotopic records of fossils from the Peterborough Member, Oxford Clay Formation (Jurassic), UK: palaeoenvironmental implications. Journal of the Geological Society of London 151, 125–138.

Armella, C., Cabaleri, N., Cagnoni, M., Ramos, A., Valencio, S., 2005a. Paleoambientes de la Formación Calabozo (Caloviano Inferior) en el Río Potimalal. In: XVI Congreso Geológico Argentino, vol. 2, pp. 117–124.

Armella, C., Cabaleri, N., Cagnoni, M., Ramos, A., Valencio, S., Panarello, H., 2005b. Caracterización paleoambiental de la Formación Calabozo, Cuenca Neuquina, provincia de Mendoza. In: II Simposio Argentino del Jurásico, pp. 1–2.

Arregui, C., Carbone, O., Martínez, R., 2011. El Grupo Cuyo (Jurásico Temprano – Medio) en la Cuenca Neuquina. In: Leanza, H.A., Arregui, C., Carbone, O., Danieli, J.C., Vallés, J.M. (Eds.), Relatorio Geología y Recursos Naturales de la provincia del Neuquén, pp. 77–89. Buenos Aires.

Bartolini, A., Baumgartner, P.O., Guex, J., 1999. Middle and Late Jurassic radiolarian paleoecology versus carbon-isotope stratigraphy. Palaeogeography, Palaeoclimatology and Palaeoecology 145, 43–60.

Brand, U., Veizer, J., 1980. Chemical diagenesis of a multicomponent carbonate system – 1: trace elements. Journal of Sedimentary Petrology 50, 1219–1236.

Burguess, P., Flint, S., Johnson, S., 2000. Sequence stratigraphic interpretation of turbiditic strata: an example from Jurassic strata of the Neuquén basin, Argentina. Geological Society of America Bulletin 112, 1650–1666.

Cabaleri, N.G., Valencio, S.A., Cagnoni, M.C., Ramos, A.M., Armella, C., Panarello, H.O., Riccardi, C.A., 2001. Facies and carbon/oxygen isotopes of the Calabozo Formation (Middle Jurassic), Arroyo La Vaina, Mendoza, Argentina. In: III South American Symposium on Isotope Geology, CD, pp. 363–366.

Cabaleri, N.G., Armella, C., Valencio, S.A., Cagnoni, M.C., Ramos, A., Valencio, S.A., 2003. Facies analysis and palaeoenvironmental interpretation of the Calabozo Formation (Middle Jurassic), Mendoza, Argentina. Revista Geológica de Chile 30, 205–221.

Cabaleri, N., Ramos, A., Cagnoni, M., Armella, C., Panarello, H., 2007. Paleoambientes de baja energía de la rampa carbonática caloviana en el morro del arroyo Calabozo, Malargüe, provincia de Mendoza. Ameghiniana 44 (R), 52.

Cagnoni, M., Ramos, A., Valencio, S., Panarello, H., Armella, C., Cabaleri, N., 2006. $\delta^{13}C$, $\delta^{18}O$ and $^{87}Sr/^{86}Sr$ of Early Callovian limestones from Cuenca Neuquina, Argentina. In: V South American Symposium on Isotope Geology, pp. 230–234.

Calvet, F., Tucker, M.E., 1988. Outer ramp carbonate cycles in the Upper Muschelkalk, Catalan Basin, NE Spain. Sedimentary Geology 57, 185–198.

Catuneanu, O., 2006. Principles of Sequence Stratigraphy. Elsevier, Amsterdam, p. 375.

Catuneanu, O., Abreu, V., Bhattacharya, J., Blum, M., Dalrymple, R., Eriksson, P., Fielding, C., Fisher, W., Galloway, W., Gibling, M., Giles, K., Holbrook, J., Jordan, R., Kendall, C., Macurda, B., Martinsen, O., Miall, A., Neal, J., Nummedal, D., Pomar, L., Posamentier, H., Pratt, B., Sarg, J.F., Shanley, K., Steel, R., Strasser, A., Tucker, M., Winker, C., 2009. Towards the standardization of sequence stratigraphy. Earth-Science Reviews 92, 1–33.

Colombié, C., Lécuyer, C., Strasser, A., 2011. Carbon- and oxygen-isotope records of palaeoenvironmental and carbonate production changes in shallow-marine carbonates (Kimmeridgian, Swiss Jura). Geological Magazine 148, 133–153.

Cristallini, E., Tomezzoli, R., Pando, G., Gazzera, C., Martínez, J.M., Quiroga, J., Buhler, M., Bechis, F., Barredo, S., Zambrano, O., 2009. Controles precuyanos en la estructura de la Cuenca Neuquina. Revista de la Asociación Geológica Argentina 65, 248–264.

Dellape, D.A., Mombrú, C., Pando, G.A., Riccardi, A.C., Uliana, M.A., Westermann, G.E.G., 1979. Edad y Correlación de la Formación Tábanos en Chacay Melehue y otras localidades de Neuquén y Mendoza. Obra Centenario Museo La Plata 5, 81–105.

Denison, R.E., Koepnick, R.B., Fletcher, A., Howell, M.W., Callaway, W.S., 1994. Criteria for retention of original seawater $^{87}Sr/^{86}Sr$ in ancient shelf limestones. Chemical Geology (Isotope Geoscience Section) 112, 131–143.

Dessanti, R.N., 1973. Descripción geológica de la Hoja 29b Bardas Blancas, provincia de Mendoza. Buenos Aires. Boletín del Servicio Nacional Minero (139), 70.

Dessanti, R.N., 1978. Descripción geológica de la Hoja 28b Malargüe, provincia de Mendoza. Buenos Aires. Boletín del Servicio Nacional Minero (149), 50.

Digregorio, J.H., Uliana, M.A., 1980. Cuenca Neuquina. In: Turner, J.C. (Ed.), Segundo Simposio de Geología Regional Argentina. Academia Nacional de Ciencias, Córdoba, pp. 985–1032.

Ditchfield, P.W., 1997. High northern palaeolatitude Jurassic–Cretaceous palaeotemperature variation: new data from Kong Karls Land, Svalbard. Palaeogeography, Palaeoclimatology and Palaeoecology 130, 163–175.

Flügel, E., 2004. Microfacies of Carbonate Rocks. Análisis, Interpretation and Application. Springer, Berlin, p. 976.

Franzese, J.R., Spalletti, L.A., 2001. Late Triassic–Early Jurassic continental extension in southwestern Gondwana: tectonic segmentation and pre break-up rifting. Journal of South American Earth Sciences 14, 257–270.

Giambiagi, L., Tunik, M., Barredo, S., Bechis, F., Ghiglione, M., Alvarez, P., Drosina, M., 2009. Cinemática de apertura del sector norte de la cuenca Neuquina. Revista de la Asociación Geológica Argentina 65, 278–292.

Groeber, P., 1946. Observaciones geológicas a lo largo del meridiano 70°. 1 Hoja Chos Malal. Sociedad Geológica Argentina, Revista (1), 117–208. Asociación Geológica Argentina, Serie C, Reimpresiones 1: 1–174 (1980).

Groeber, P., Stipanicic, P.N., Mingramm, A., 1953. Mesozoico. In: Geografía de la República Argentina Primera Parte. Sociedad Argentina de Estudios Geográficos, p. 541.

Grotzinger, J.P., Fike, D.A., Fischer, W.W., 2011. Enigmatic origin of the largest-known carbon isotope excursion in Earth's history. Nature Geoscience 4, 285–292.

Gulisano, C.A., 1981. El Ciclo Cuyano en el norte del Neuquén y sur de Mendoza. In: Actas VIII Congreso Geológico Argentino, vol. 3, pp. 579–592.

Gulisano, C.A., Gutiérrez Pleimling, A.R., 1995. Field Guide. The Jurassic of the Neuquén Basin, Mendoza Province. Secretaría de Minería de la Nación. Pub. N° 159 y Asociación Geológica Argentina, Serie E, N° 3, p. 103.

Gulisano, C.A., Hinterwimmer, G., Setiembre 1986. Facies deltaicas del Jurásico Medio en el oeste del Neuquén. Boletín de Informaciones Petroleras, 2–31.

Gulisano, C.A., Gutiérrez Pleimling, A.R., Digregorio, R.E., 1984. Esquema estratigráfico de la secuencia jurásica del oeste de la provincia del Neuquén. In: Actas IX Congreso Geológico Argentino, vol. 1, pp. 236–259.

Hallam, A., 1983. Early and Mid-Jurassic molluscan biogeography and the establishment of the central Atlantic seaway. Palaeogeography, Palaeoclimatology and Palaeoecology 43, 181–193.

Howell, J.A., Schwarz, E., Spalletti, L.A., Veiga, G.D., 2005. The Neuquén Basin: an overview. In: Veiga, G.D., Spalletti, L.A., Howell, J.A., Schwarz, E. (Eds.), The Neuquén Basin, Argentina: A Case Study in Sequence Stratigraphy and Basin Dynamics. Geological Society of London, Special Publications, vol. 252, pp. 1–14.

Jacobsen, S., Kaufman, A., 1999. The Sr, C and O isotopic evolution of Neoproterozoic seawater. Chemical Geology 161, 37–57.

Jenkyns, H.C., Jones, C.E., Gröcke, D.R., Hesselbo, S.P., Parkinson, D.N., 2002. Chemostratigraphy of the Jurassic System: applications, limitations and implications for palaeoceanography. Journal of the Geological Society of London 159, 351–378.

Leanza, H.A., 2009. Las principales discordancias del Mesozoico de la Cuenca Neuquina según observaciones de superficie. Revista del Museo Argentino de Ciencias Naturales 11, 145–184. Buenos Aires.

Leanza, H.A., Rosenfeld, U., Volkheimer, W., Zeiss, A., 2000. Facies Evolution of the Mesozoic Neuquén Basin (Argentina) in Space and Time. SH1 Sonderheft ZAG, Hannover, pp. 103–109.

Leanza, H.A., Mazzini, A., Corfu, F., Llambías, E.J., Svensen, H., Planke, S., Galland, O., 2012. The Chachil limestone (Pliensbachian-earliest Toarcian) Neuquén Basin, Argentina: U–Pb age calibration and its significance on the Early Jurassic evolution of southwestern Gondwana. Journal of South American Earth Sciences. http://dx.doi.org/10.1016/j.jsames.2012.07.012.

Legarreta, L., 2002. Eventos de desecación en la cuenca Neuquina. Depósitos continentales y distribución de hidrocarburos. In: V Congreso de Exploración de Hidrocarburos, Mar del Plata, Argentina, CD, 20 pp..

Legarreta, L., Gulisano, C.A., 1989. Análisis estratigráfico de la Cuenca Neuquina (Triásico superior–Terciario inferior, Argentina). In: Chebli, G., Spalletti, L. (Eds.), Cuencas Sedimentarias Argentinas. Serie de Correlación Geológica, vol. 6. Instituto Superior de Correlación Geológica, Universidad Nacional de Tucumán, Argentina, pp. 221–244.

Legarreta, L., Uliana, M.A., 1996. The Jurassic succession in west-central Argentina: stratal patterns, Sequence and paleogeographic evolution. Palaeogeography, Palaeoclimatology and Palaeoecology 120, 303–330.

Legarreta, L., Uliana, M.A., 1999. El Jurásico y Cretácico de la Cordillera Principal y de la Cuenca Neuquina. 1. Facies Sedimentarias. In: Caminos, R. (Ed.), Geología Argentina. Servicio Geológico y Minero Argentino, Anales, vol. 29, pp. 399–416.

Legarreta, L., Gulisano, C.A., Uliana, M.A., 1993. Las secuencias sedimentarias jurásico-cretácicas. In: Relatorio XII Congreso Geológico Argentino, pp. 87–114.

Legarreta, L., Laffitte, G., Minniti, S., 1999. Cuenca Neuquina: múltiples posibilidades en las series jurásico-cretácicas del depocentro periandino. In: IV Congreso de Exploración y Desarrollo de Hidrocarburos, Tomo I. IAPG, pp. 145–175.

Mazzini, A., Svensen, H., Leanza, H.A., Corfu, F., Planke, S., 2010. Early Jurassic shale chemostratigraphy and U–Pb ages from the Neuquén Basin (Argentina): implications for the Toarcian Oceanic Anoxic Event. Earth and Planetary Science Letters 297, 633–645.

Mc ILroy, D., Flint, S., Howell, J., Timms, N., 2005. Sedimentology of the tide-dominates Jurassic Lajas Formation, Neuquén Basin. In: Veiga, G.D., Spalletti, L.A., Howell, J.A., Schwarz, E. (Eds.), The Neuquén Basin, Argentina: A Case Study in Sequence Stratigraphy and Basin Dynamics. Geological Society of London, Special Publications, vol. 252, pp. 83–107.

McCrea, J.M., 1950. On the isotopic chemistry of carbonates and a paleotemperature scale. Journal of Chemical Physics 18, 849–857.

Morettini, E., Santantonio, M., Bartolini, A., Cecca, F., Baumgartner, P., Hunziker, J., 2002. Carbon isotope stratigraphy and carbonate production during the Early–Middle Jurassic: examples from the Umbria–Marche-Sabina Apennines (central Italy). Palaeogeography, Palaeoclimatology and Palaeoecology 184, 251–273.

Osleger, D., 1991. Subtidal carbonate cycles: implications for allocyclic vs. autocyclic controls. Geology 19, 917–920.

Pemberton, S.:G., Mac Eachern, J.A., Frey, R.W., 1992. Trace fossil facies models. Environmental and allostratigraphic significance. In: Walker, R.G., James, N.P. (Eds.), Facies Models: A Response to Sea Level Changes. Geological Association of Canada, pp. 47–72.

Read, J.F., 1985. Carbonate platform facies models. American Association of Petroleum Geologists Bulletin 69, 1–21.

Riccardi, A.C., 1984. Las asociaciones de Amonitas del Jurásico y Cretácico de la Argentina. In: Actas IX Congreso Geológico Argentino, vol. 4, pp. 559–595.

Riccardi, A.C., Westermann, G.E.G., 1991. Middle Jurassic Ammonoid fauna and Biochronology of the Argentine-Chilean Andes. Part III: Bajocian-Callovian Eurycephalitinae, Stephanoceratoceae. Part IV: Bathonian-Callovian Reineckeiidae. Palaeontographica A 216 (1–6), 1–145.

Riccardi, A.C., Damborenea, S., Manceñido, M.O., Ballent, S.C., 1999. El Jurásico y Cretácico de la Cordillera Principal y de la Cuenca Neuquina. In: Caminos, R.

(Ed.), Geología Argentina, Bioestratigrafía. Servicio Geológico y Minero Argentino, Anales, vol. 29, pp. 419–433.
Riccardi, A.C., Leanza, H.A., Damborenea, S.E., Manceñido, M.O., Ballent, S.C., Zeiss, A., 2000. Marine Mesozoic Bioestratigraphy of the Neuquén Basin. SH1 Sonderheft ZAG, Hannover, pp. 103–109.
Riding, J.B., Quattrocchio, M.E., Martínez, M.A., 2011. Mid Jurassic (Late Callovian) dinoflagellate cysts from the Lotena Formation of the Neuquén Basin, Argentina and their palaeogeographical significance. Review of Palaeobotany and Palynology 163, 227–236.
Rosales, I., Robles, S., Quesada, S., 2004. Elemental and oxygen isotope composition of Early Jurassic belemnites: salinity vs. temperature signals. Journal of Sedimentary Research 74, 342–354.
Spalletti, L., Franzece, J., Matheos, S., Schwarz, E., 2000. Sequence stratigraphy of a tidally-dominated carbonate–siliciclastic ramp: the Tithonian of the southern Neuquén Basin, Argentina. Journal of the Geological Society of London 157, 433–446.
Stipanicic, P.N., 1966. El Jurásico en Vega de la veranada (Neuqué n), el Oxfordense y el diastrofismo Divesiano (Agassiz-Yaila) en Argentina. Revista de la Asociación Geológica Argentina 20, 403–478.
Stipanicic, P.N., 1969. El avance en los conocimientos del Jurásico argentino a partir del esquema de Groeber. Revista de la Asociación Geologica Argentina 24, 367–388.
Tucker, M.E., Wright, V.P., 1990. Carbonate Sedimentology. Blackwell Science, Oxford, p. 482.
Uliana, M.A., Biddle, K.T., 1988. Mesozoic–Cenozoic paleogeographical and geodynamic evolution of southern South America. Revista Brasileira de Geociencias 18, 172–190.
Uliana, M.A., Biddle, K., Cerdán, J., 1989. Mesozoic extension and the formation of Argentina sedimentary basins. In: Tankard, A.J., Balkwill, H.R. (Eds.), Extensional Tectonics and Stratigraphy of the North Atlantic Margin. American Association of Petroleum Geologists, Memoir, vol. 46, pp. 599–613. Tulsa.
Uliana, M.A., Arteaga, M.E., Legarreta, L., Cerdán, J., Peroni, G., 1995. Inversion structures and hydrocarbon occurrence in Argentina. Geological Society Special Publication 88, 211–233. Tulsa.
Valencio, S.A., Ramos, A.M., Cagnoni, M.C., Panarello, H.O., Cabaleri, N.G., Armella, C., 2003. Isotope signal of the Middle Jurassic carbonate ramp of Calabozo Formation, at arroyo El Plomo, Mendoza, Argentina. In: IV South American Symposium on Isotope Geology. Salvador, Bahia. Brasil. CD and Actas, pp. 409–412.
Veizer, J., Ala, D., Azmy, K., Bruckschen, P., Buhl, D., Bruhn, F., Carden, G.A.F., Diener, A., Ebneth, S., Godderis, Y., Jasper, T., Korte, C., Pawellek, F., Podlaha, O.G., Strauss, H., 1999. $^{87}Sr/^{86}Sr$, $\delta^{13}C$ and $\delta^{18}O$ evolution of Phanerozoic seawater. Chemical Geology 161, 59–88.
Volkheimer, W., 1970. Neuere Ergerbnisse der Anden-Stratigraphie von süd-Mendoza (Argentinien) und benachbarter Gebiete und Bemerkungen zur Klimageschichte des süddlichen Andenraums. Geologische Rundschau 59 (3), 1098–1100.
Weaver, C.E., 1931. Paleonttology of the Jurassic and Cretaceous of West Central Argentinsa. In: Memoir University of Washington, vol. 1, pp. 1–496. Seatle.
Westermann, G.E.G., Riccardi, A.C., 1985. Middle Jurassic ammonite evolution in the Andean Province and emigration to Tethys. In: Bayer, U., Seilacher, A. (Eds.), Sedimentary and Evolutionary Cycles. Lecture Notes in Earth Sciences, vol. 1, pp. 6–34.
Wilson, J.L., 1975. Carbonate Facies in Geologic History. Springer-Verlag, Berlin, p. 471.
Wissler, L., Funk, H., Weissert, H., 2003. Response of Early Cretaceous carbonate platforms to changes in atmospheric carbon dioxide levels. Palaeogeography, Palaeoclimatology and Palaeoecology 200, 187–205.
Wright, V.P., Burchette, T.P., 1996. Shallow-water carbonate environments. In: Reading, H.G. (Ed.), Sedimentary Environments: Processes, Facies and Stratigraphy. Blackwell Sciences, Oxford, pp. 325–394.
Yrigoyen, M.R., 1979. Cordillera principal. In: Turner, J.C. (Ed.), 1979. Segundo Simposio de Geología regional Argentina, vol. 1. Academia Nacional de Ciencias, pp. 651–694.
Žák, K., Košťák, M., Man, O., Zakharov, V.A., Rogov, M.A., Pruner, P., Rohovec, J., Dzyuba, O.S., Mazuch, M., 2011. Comparison of carbonate C and O stable isotope records across the Jurassic/Cretaceous boundary in the Tethyan and Boreal Realms. Palaeogeography, Palaeoclimatology and Palaeoecology 299, 83–96.